ACVR1 antibodies exacerbate heterotopic ossification in fibrodysplasia ossificans progressiva (FOP) by activating FOP-mutant ACVR1

Senem Aykul[1]*
Lily Huang[1]*
Lili Wang[1]
Nanditha Das[1]
Sandra Reisman[1]
Yonaton Ray[1]
Qian Zhang[1]
Nyanza Rothman[1]
Kalyan C. Nannuru[1]
Vishal Kamat[1]
Susannah Brydges[1]
Luca Troncone[2]
Laura Johnsen[1]
Paul B. Yu[2]
John Lees-Shepard[1]
Kevin Schutz[3]
Andrew J. Murphy[1]
Aris N. Economides[1]†
Vincent Idone[1]†
Sarah J. Hatsell[1]†

*Indicates equal contribution.
†Indicates equal contribution; to whom correspondence should be addressed.
Sarah.hatsell@regeneron.com, Vincent.idone@regeneron.com, aris@regeneron.com

[1]Regeneron Pharmaceuticals Inc, 777 Old Saw Mill River Road, Tarrytown, NY 10591, USA.
[2]Department of Medicine, Cardiovascular Division, Brigham and Women's Hospital, Harvard Medical School, Boston, MA 02114, USA.
[3]Adimab, 7 Lucent Dr, Lebanon, NH 03766, USA.

Abstract

Fibrodysplasia ossificans progressiva (FOP) is a rare genetic disorder whose most debilitating pathology is progressive and cumulative heterotopic ossification (HO) of skeletal muscles, ligaments, tendons, and fascia. FOP is caused by amino acid-altering mutations in ACVR1, a type I BMP receptor. The mutations occur in the region encoding the intracellular domain of ACVR1 and bestow FOP-mutant ACVR1 with the neofuction of recognizing Activin A as an agonistic ligand. (In contrast, Activin A antagonizes BMP signaling from wild type ACVR1.) This neofuction is required for HO in FOP as inhibition of Activin A stops the initiation and progression of heterotopic bone lesions in FOP. These results unequivocally demonstrated that HO in FOP is dependent on activation of FOP-mutant ACVR1 by ligand and set the stage to explore ACVR1-blocking antibodies as an additional potential therapeutic for FOP. Surprisingly, ACVR1 antibodies stimulate – rather than inhibit – HO and induce Smad1/5/8 phosphorylation of FOP-mutant ACVR1. This property is restricted to FOP-mutant ACVR1, as signaling by wild type ACVR1 is inhibited by these antibodies, as is trauma-induced HO. These results uncover yet an additional novel property of FOP-mutant ACVR1 and indicate that anti-ACVR1 antibodies should not be considered as a therapeutic strategy for FOP.

Introduction

Fibrodysplasia ossificans progressiva (FOP) (OMIM #135100) is a rare, autosomal dominant disorder characterized by congenital skeletal dysplasias and progressive and cumulative heterotopic ossification (HO) of skeletal muscles, tendons, ligaments, and fascia (1). FOP arises from amino acid-altering mutations in the cytoplasmic domain of the type I Bone Morphogenetic Protein (BMP) receptor Activin A Receptor Type 1 (ACVR1), with the most common mutation being c.617G>A, altering Arginine 206 to a Histidine (R206H), occurring in approximately 95% of patients (2), but with multiple additional FOP-causing variants in the GS and kinase domains of ACVR1 (3, 4).

This discovery sparked the question of what property do these amino acid-altering mutations impart to ACVR1. Their location in the intracellular domain of this BMP receptor indicated that changes in ligand binding properties were unlikely, and therefore the focus was placed on the variants' signaling properties (2, 3). Initial investigations proposed that FOP-mutant ACVR1 causes HO by being hyperactivated by BMP ligands or by displaying a certain level of constitutive activity (reviewed in (5, 6)). However, these investigations did not utilize genetically accurate *in vivo* models of FOP and did not query the physiological relevance of their findings. Using a mouse model of FOP, *Acvr1*$^{[R206H]FlEx/+}$*; GT(ROSA26)Sor*$^{CreERT2/+}$, which models the most common FOP-causing variant of ACVR1, and in which HO is triggered by systemic

treatment with tamoxifen in addition to soft tissue palpitations, we demonstrated that HO in FOP requires activation of FOP-mutant ACVR1 by Activin A (7). Furthermore, we demonstrated that Activin A normally functions as an antagonist of BMP signaling via wild type ACVR1, whereas it is perceived by FOP-mutant ACVR1 as an agonist, and activates signaling just like a BMP (7, 8). Inhibition of Activin A using a monoclonal antibody completely abrogates the occurrence of new HO lesions and halts growth of nascent HO lesions, demonstrating that activation of FOP-mutant ACVR1 by Activin is required for HO in FOP mice (7, 9). These results have been independently reproduced (10-12), firmly establishing the requirement of Activin A as an obligate factor for HO in FOP.

The finding that HO in FOP is ligand-dependent suggested that antibodies that block ligand-induced activation of ACVR1 could be efficacious despite the disease-causing mutation being in the intracellular domain of this receptor. We therefore developed antibodies to ACVR1 that block ligand-induced signaling and tested these antibodies in FOP mice. Surprisingly, although these ACVR1 antibodies block ligand-induced signaling *in vitro*, they activate FOP-mutant ACVR1 (and do so independently of ligand) and exacerbate (rather than block) HO in FOP mice. This novel property of FOP-mutant ACVR1 – to be activated as a result of antibody-mediated dimerization (whereas wild type ACVR1 is not) – present an additional novel property for this mutant receptor. More importantly, these results indicate that ACVR1 antibodies should not be considered as a therapeutic strategy in FOP.

Results

ACVR1 blocking antibodies inhibit ligand induced signaling through both wild type ACVR1 and ACVR1[R206H] *in vitro*

Given the high level of amino acid sequence identity between mouse and human ACVR1, we utilized an *in vitro* yeast-based platform (13) to isolate human-murine ACVR1 cross-reactive antibodies. Three lead antibodies – Mab 1, Mab 2, and Mab 3 – were selected as they display a high affinity for both human and mouse ACVR1 (Supplemental Table 1 and Supplemental Table 2), lack binding to related BMP receptors (Supplemental Table 3), and block signaling. More specifically, these antibodies block BMP7-induced Smad1/5/8 signaling as measured by ALP activity in W20 cells overexpressing wild type ACVR1 (Supplemental Figure 1A, B), as well as BMP7- and Activin A-induced signaling in Hek293 cells overexpressing ACVR1[R206H] as measured by BRE-luciferase activity (Figure 1A, B).

ACVR1 blocking antibodies increase HO in FOP mice

We have previously demonstrated that Activin A signaling through ACVR1[R206H] is required for HO in FOP mice and that its inhibition completely abrogates the initiation and progression of HO (7). We therefore reasoned that ACVR1 antibodies that block ligand-induced signaling through ACVR1[R206H] should also be efficacious in this model. Unexpectedly, when ACVR1 antibodies were dosed prophylactically at the time of initiation of the model, HO was greatly enhanced compared to the level of HO observed in FOP mice treated with an isotype control antibody (Figure 1C, D). This suggested that these antibodies were activating rather than blocking the FOP-mutant ACVR1 *in vivo*. This property was shared by all three Mabs. Since these Mabs bind ACVR1 at different epitopes (Supplemental Table 4), the ability of these Mabs to exacerbate HO in FOP is a shared property of these antibodies and does not depend on binding ACVR1's extracellular domain at any particular site.

ACVR1 antibodies block traumatic HO in WT mice

To confirm that ACVR1 antibodies are able to block WT ACVR1 in the setting of HO *in vivo*, we tested Mab 1 in the burn tenotomy model of trauma-induced HO (tHO) in WT mice (14). Consistent with previous data (15) either Mab 1 or ALK3-Fc (which blocks osteogenic BMPs), were able to reduce though not completely ameliorate tHO when dosed at the same time as induction of the model via burn combined with tenotomy (Supplemental Figure 2). These results confirm that antibody-mediated inhibition of ACVR1 can block HO but only outside of FOP.

Effect of ACVR1 antibodies on iron homeostasis in FOP mice is consistent with activating ACVR1[R206H]

We next tested whether this apparent activation of ACVR1[R206H] by ACVR1 antibodies extends to other tissues, rather than being limited to HO, focusing on iron homeostasis, where the role of ACVR1 is well established (16). Hence, we measured the effect of ACVR1 antibodies on iron homeostasis using Hepcidin levels as a surrogate, as well as serum iron levels directly. Hepcidin expression is upregulated by BMP2 and BMP6 signaling through ACVR1/BMPR1A in hepatocytes (16-18). Inhibition of ACVR1-mediated signaling is expected to decrease hepcidin levels (and increase serum iron), whereas its activation is expected to increase hepcidin levels (and decrease serum iron). We therefore used hepcidin production by the liver, as measured by circulating hepcidin levels, to determine the effect of ACVR1 antibodies on ACVR1-mediated signaling. *Acvr1*$^{+/+}$*; GT(ROSA26)Sor*$^{CreERT2/+}$ (WT) or *Acvr1*$^{[R206H]/+}$*; GT(ROSA26)Sor*$^{CreERT2/+}$ (FOP) mice were dosed with Mab 1 and circulating hepcidin was measured. Treatment with Mab 1 resulted in a decrease of hepcidin in WT mice (Figure 2A), whereas it increased hepcidin levels in FOP mice (Figure 2B). The results obtained with hepcidin were mirrored by serum iron levels

(Figure 2C, D). These data demonstrate that the same ACVR1 antibody inhibits wild type ACVR1 but activates ACVR1[R206H] *in vivo* and extend its physiological effects to a system other than HO.

ACVR1 Mabs activate whereas Fabs block ACVR1[R206H] signaling

Our results are consistent with a model wherein ACVR1 antibodies block ligand binding, and simultaneously activate FOP-mutant ACVR1 by dimerizing it. Furthermore, this effect is specific to FOP-mutant ACVR1 – WT ACVR1 is not activated when dimerized by ACVR1 antibodies. One prediction of this model is that monomeric versions of ACVR1 antibodies should block activation of both ACVR1[R206H] and WT ACVR1. To test this idea, we generated Fabs of two of the ACVR1 antibodies (Mab 2 and Mab 3), Fab 2 and Fab 3, established that they block ligand-induced ACVR1-mediated signaling *in vitro* (Supplemental Figure 1C, D, Supplemental Figure 3), and then tested whether they are able to stop HO in FOP mice. In order to overcome the short *in vivo* half-life of Fabs, we used hydrodynamic delivery (HDD) to deliver plasmids encoding the Fabs to hepatocytes, hence enabling continuous production of the Fabs. These two Fabs significantly reduced HO in FOP mice (Figure 3A, B) compared to a control antibody thereby confirming that ACVR1 Fabs can inhibit ACVR1[R206H] *in vivo*.

In parallel with these *in vivo* experiments we explored the effect of an ACVR1 Mab and the corresponding Fab directly on signaling *in vitro*, focusing on two types of cells with endogenous expression of ACVR1: *Acvr1*$^{[R206H]/+}$*; GT(ROSA26)Sor*$^{CreERT2/+}$ mES cells, and fibroadipogenic progenitor cells (FAPs), i.e. the cells that give rise to HO in FOP mice (11, 12). Consistent with the *in vivo* data, Mab 2 was able to induce Smad1/5/8 phosphorylation in the absence of exogenously added ligand, albeit to a lower level than Activin A (Figure 3C, Supplemental Figure 4). In contrast, Mab 2 could not induce Smad1/5/8 signaling in cells expressing WT ACVR1 (Supplemental Figure 5). As expected, Fab 2 failed to activate Smad1/5/8 signaling in ACVR1[R206H]-expressing cells but was able to block Activin A-induced signaling. Identical results were obtained with another FOP-causing variant, ACVR1[R258G] (19) (Supplemental Figure 5). These results firmly establish that FOP-mutant ACVR1 is activated when dimerized by ACVR1 antibodies, resulting in a signal that is lower than that obtained by Activin A, but adequate to exacerbate HO and reduce serum iron in FOP mice.

Lastly, we investigated whether the dimerization has to take place via interactions with either ligand or antibody binding to the extracellular domain of ACVR1[R206H] or whether other means of dimerization would also activate signaling. We turned to a different method of inducing dimerization, one that utilizes a small molecule-controlled dimerization domain, DmrB

(20). We generated cells expressing either WT human ACVR1 or human ACVR1[R206H] bearing a DmrB dimerizing domain fused to their C-termini. After demonstrating that each fusion retains its response to physiological ligands (i.e. BMP6 for WT ACVR1-DmrB, and ACVR1[R206H]-DmrB; and Activin A for ACVR1[R206H]-DmrB) (Supplemental Figure 6A, B), we tested their response to the small molecule dimerizer. Whereas WT ACVR1-DmrB failed to respond, dimerization of ACVR1[R206H]-DmrB activated signaling (Supplemental Figure 6C, D). The signal remains unaltered when ACVR2B-Fc (which would bind any endogenous ligands that might be present) was included, indicating that the observed response is not dependent on any endogenous ligands (Figure 6D). These results further highlight the fact that simple dimerization of ACVR1[R206H] activates that receptor, in stark contrast to WT ACVR1 wherein activation of signaling requires interaction with specific BMPs.

ACVR1 antibody-induced activation of ACVR1[R206H] is independent of Activin A

Given that the ACVR1 antibodies block interaction of ACVR1 with its ligands, we considered it unlikely that the ACVR1 antibody-induced signaling involves Activin A, the obligate ligand for HO in FOP. Nonetheless, to exclude this possibility we tested whether antibody activation of ACVR1[R206H] is dependent on Activin A both in cells and in FOP mice. In both mES cells and FAPs the ability of Mab 2 to activate signaling is Activin A independent (Figure 3C, Supplemental Figure 4) as treatment of these cells with both an Activin A blocking antibody and Mab 2 resulted in Smad 1/5/8 phosphorylation to similar levels as Mab 2 alone. To confirm that HO observed in FOP mice treated with ACVR1 antibodies is independent of Activin A, we tested whether ACVR1 antibody-exacerbated HO persisted in FOP mice in the presence of Activin A blocking antibodies. Two Activin A antibodies were investigated: REGN2476, which blocks binding of Activin A to both type I and type II receptors, and REGN2477, which allows binding of Activin A to type II receptors but inhibits signaling by blocking engagement with type I receptors (8) (Supplemental Figure 13). Both of these antibodies completely inhibit HO formation in FOP mice when dosed prophylactically (7, 9) (Figure 3D). However, neither of these antibodies were able to ameliorate the increased HO seen with the ACVR1 antibody demonstrating that this outcome is independent of Activin A (Figure 3D).

ACVR1 antibody-induced activation of ACVR1[R206H] requires type II receptors

The fact that FOP-mutant ACVR1 can be activated by dimerization mediated by ACVR1 antibodies even in the absence of extracellular ligands (Supplemental Figure 6), prompted us to investigate whether type II receptors play a role in this process. For these experiments, we engineered *Acvr1*$^{[R206H]/+}$*; GT(ROSA26)Sor*$^{CreERT2/+}$ mES cell lines lacking *Acvr2a* and *Acvr2b*, or

Bmpr2, or all three of these type II receptor genes. Prior to use, these mES cell lines were tested for expression of ACVR1, ACVR2A, ACVR2B, and BMPR2 (Supplemental Figures 7, and 8), in order to check that the expression of these genes was not altered except as intended. Subsequently, these mES cell lines were treated with Activin A or BMPs or the ACVR1 antibody Mab1. Loss of BMPR2 did not have any appreciable effect on signaling either by the ligands or Mab1. However, loss of ACVR2A and ACVR2B rendered these cells unresponsive to Activin A as well as Mab1 (Figure 4A), indicating that type II receptors are required for signaling even if they are not involved in a ligand-induced complex. Our results are in agreement with published reports that type II receptors are required for signaling by ACVR1, independent of ligand binding (21-23).

This result also suggested that type II receptors must exist in preformed heterodimeric complexes with ACVR1. Such complexes indeed exist, as immunoprecipitation of a myc-tagged ACVR1 coimmunoprecipates ACVR2B (Figure 4B, Supplementary Figure 9). These preformed complexes are not particular to ACVR1[R206H] as they also form with WT ACVR1. Similar preformed heterodimeric complexes have been observed between other type I and type II BMP receptors (24), and hence appear to be a general property of this class of receptor proteins.

ACVR1 antibodies also activate human ACVR1[R206H]

Human and mouse ACVR1 differ by 5 amino acids in their mature form (Supplemental Figure 10). Two of these amino acids are found in the intracellular domain, specifically at positions 182 and 330. It has been reported that the amino acid at position 330 is a key determinant of the response of ACVR1 to ACVR1 antibodies *in vitro*, and more specifically that proline at 330 renders human ACVR1[R206H] resistant to activation by dimerization (25). This stands in contrast to mouse ACVR1, which has a serine at position 330.

To investigate this reported difference *in vivo* we altered serine 330 to a proline and humanized the extracellular domain of *Acvr1*$^{[R206H]FlEx}$ *to produce Acvr1*$^{huecto[R206H]FlEx;[S330P]/+}$*; GT(ROSA26)Sor*$^{CreERT2/+}$ mES cells and mice. As with the original mouse model, we induced the FOP genotype in mice through treatment with tamoxifen to generate their FOP counterparts (FOP$^{[S330P]}$ mice). We then dosed both FOP and FOP$^{[S330P]}$ mice with Mab 1 simultaneously with initiation of the model. As expected, Mab 1 induced severe HO in FOP mice that necessitated euthanization after 3 weeks. In FOP$^{[S330P]}$ mice, ACVR1 antibody treatment also increased HO compared to isotype control, albeit to a lower level than that seen in FOP mice (Figure 5A, B). This difference in degree of activation was mirrored in the change of serum iron levels, which were more reduced in FOP mice than in FOP$^{[S330P]}$ mice (Supplemental Figure 11). Nonetheless,

both effects – an increase in HO and a decrease in serum iron – were observed with Mab 1 treatment of FOP[S330P] mice, mirroring the results obtained with FOP mice.

However, *in vitro*, antibody-induced dimerization of ACVR1[huecto;R206H;S330P] did not result in detectable levels of Smad1/5/8 phosphorylation, when Mab 1 was the dimerizing antibody. We attributed this to the fact that Mab 1 recognizes both the WT and FOP mutant allele and therefore induces dimeric complexes of WT/WT, WT/FOP and FOP/FOP ACVR1, and hence potentially resulting in a situation where only 25% of FOP-mutant ACVR1 would transduce signal. We reasoned that an ACVR1 antibody that recognizes only human ACVR1 (Supplemental Table 1 and 2) and hence promotes solely the formation of ACVR1[huecto;R206H;S330P] homodimers would elevate the level of signaling to the point that it can be detected. Indeed, using such an antibody as the dimerizing antibody resulted in induction of Smad1/5/8 phosphorylation (Figure 5C). This result is consistent with that obtained when dimerizing human ACVR1[R206H]-DmrB (Figure 6C, D). Hence, these results indicate that the property of ACVR1[R206H] to be activated when dimerized by ACVR1 antibodies is conserved between humans and mice. Although it appears that human ACVR1[R206H] is less active than its mouse counterpart, these results strongly caution against the use of ACVR1 antibodies as a therapeutic for blocking HO in FOP, because they clearly induce more HO than that observed when FOP[S330P] mice are dosed with a control antibody (akin to placebo) and may also lead to anemia.

Discussion

In our quest to develop disease modifying therapies for FOP, we sought to understand how FOP-mutant ACVR1 drives HO. We engineered a genetically accurate mouse model of FOP and have relied on this model to explore the pathophysiology of FOP and place findings from *in vitro* experiments into a physiological context. Using this approach, we discovered an unusual property of FOP-mutant ACVR1, that it is activated by its own natural antagonist, Activin A (7). Whereas WT ACVR1 forms non-signaling complexes with Activin A and the corresponding type II receptors (8), FOP-mutant ACVR1 is activated by Activin A. This neofunction is essential for HO in FOP, as inhibition of Activin A using monoclonal antibodies ameliorates the initiation and progression of heterotopic bone lesions in FOP mice (7, 9, 12). These results culminated in a clinical trial – LUMINA-1 (NCT03188666) – to test the safety and efficacy of REGN2477 (an Activin A Mab) in FOP.

In addition, these results proved unequivocally the ligand-dependence of HO in FOP (with the 'culprit' ligand being Activin A). Based on this, we reasoned that inhibition of ligand-induced signaling using antibodies to ACVR1 may present an additional potential therapeutic approach.

To this effect, we generated a set of ACVR1 Mabs that block signaling from ACVR1 *in vitro*. Surprisingly, these Mabs exacerbate HO in FOP mice, and activate Smad1/5/8 phosphorylation in cells expressing FOP-mutant ACVR1 *in vitro*, in the absence of ligands. Furthermore, this effect is not restricted to HO, as ACVR1 antibodies also alter iron homeostasis in a manner consistent with activation of ACVR1[R206H]: they increase hepcidin levels and reduce serum iron levels, phenocopying activation of signaling via ACVR1. At first glance, these results contradict our initial bioassay data (Figure 1), where we utilized cells overexpressing ACVR1[R206H] and a BRE-luciferase assay as a surrogate for activation of the Smad1/5/8 pathway to screen for Mabs with the desired properties. Such a discrepancy has been noted by others (23). Irrespective of the reasons for this discrepancy, it is clear that in physiological settings ACVR1[R206H] is activated by ACVR1 Mabs. This observation also holds for an additional FOP-causing variant of ACVR1, 258G; however, we have yet to test any other ACVR1 variants documented to cause FOP (4).

Although the level of antibody induced activation is well below that seen with ligand induced activation, the antibodies greatly exacerbate HO in FOP mice. We postulate that this is due to a more widespread and sustained availability of an antibody in contrast to a local and immediate but transient induction of Activin A after muscle injury (26). We perhaps see evidence of this reflected in the characteristics of HO lesions in antibody treated mice (Supplemental Figure 12). At two weeks post injury, HO lesions in ACVR1 antibody treated mice appear larger but less mature than that seen in isotype control treated mice, suggesting that the initial injury induced Activin A signal is inhibited and replaced with the weaker but more widespread antibody induced signal in the injured muscle. However, subsequently in ACVR1 antibody treated mice the HO process remains far more active than in isotype control treated mice suggesting that the endogenous Activin A signal has decreased but the ACVR1 antibody is still abundant and, by activating FOP-mutant ACVR1, can continue to direct FAPs down an endochondral lineage (11, 12).

Our data also supports a requirement for some degree of muscle trauma that necessitates a repair response to initiate HO in FOP. This repair response is likely to be required to both provide activin A but also to activate and expand FAPs so that they can respond to activin A and differentiate down an endochondral lineage. If activation of FAPs by injury was not required, then we would expect ACVR1 antibodies to induce HO much more widely when administered to FOP mice. This data is also consistent with the phenotype seen in the mouse model expressing ACVR1[Q207D], an engineered constitutively active and ligand-independent variant of ACVR1. In these mice, injury is also required to induce HO (27), indicating that ACVR1-mediated signaling leads to HO only if it takes place within cells that are primed to respond.

Activation of FOP-mutant ACVR1 by ACVR1 Mabs is a result of dimerization of this receptor by these naturally bivalent Mabs. Consistent with this notion, ACVR1 Fabs, which are naturally monovalent and hence cannot dimerize ACVR1, block HO in FOP mice and fail to activate ACVR1[R206H] *in vitro*. Further evidence that dimerization is adequate to activate FOP-mutant ACVR1 is that other methods of dimerization produce the same result. For example, activation is also achieved when an ACVR1[R206H]-DmrB fusion protein is dimerized by the corresponding small molecule. Furthemore, dimerization of an N-terminally myc-tagged ACVR1[R206H] using a myc antibody activates signaling, indicating that the dimerizing antibody need not bind to a region of ACVR1 that is involved in ligand engagement (data not shown).

The responsiveness of FOP-mutant ACVR1 to ACVR1 antibodies is conserved between mouse and human ACVR1[R206H], contrary to an initial report that this might not be the case (25). This report attributed the apparent resistance of human ACVR1[R206H] to dimerization-induced activation to the presence of a proline at position 330, rather than serine in mouse ACVR1[R206H]. We show here that human ACVR1[R206H] is activated by ACVR1 antibodies, but the resulting signal is weaker than that generated by mouse ACVR1[R206H]. In $FOP^{[S330P]}$ mice ACVR1 antibodies exacerbate HO, though to a lesser degree than when engaging mouse ACVR1[R206H], mirroring the lower activity displayed by human ACVR1[R206H] *in vitro*.

Although activation of FOP-mutant ACVR1 by antibodies occurs in the absence of ligands, we demonstrate that type II receptors are still required. Type II receptors appear to be associated with ACVR1 (both WT and FOP-mutant) in preformed, ligand-independent complexes. Our findings mirror observations made for BMPR1A or BMPR1B and BMPR2 (24). Given that these complexes are not specific to FOP-mutant ACVR1, it is remains unclear as to why ACVR1 antibodies do not also activate WT ACVR1. Hence, antibody-induced dimerization of ACVR1 appears to be equivalent to Activin A-induced homodimerization of ACVR1: neither one activates WT ACVR1 whereas as both activate FOP-mutant ACVR1.

Overall, our results indicate that FOP-mutant ACVR1 likely exists in a “permissive” conformation wherein it can be activated by simple dimerization. Normally dimerization of ACVR1 is brought about by ligands, an interaction that naturally requires participation of type II receptors. ACVR1 antibodies bypass this requirement at the level of dimerization, but type II receptors are still required for signaling and are able to participate because they exist in preformed (and ligand-independent) heterocomplexes with ACVR1. In spite of these insights, the molecular mechanism by which stoichiometrically identical complexes (i.e. ACVR1•Activin A•type II receptor, which does not signal, versus $ACVR1^{FOP}$•Activin A•type II receptor, or ACVR1•BMP•type II receptor, both of which transduce signal) result in these two opposite outcomes remains an open question.

Taken together, our results reveal an additional novel property of FOP-mutant ACVR1, that it can be activated by ACVR1 antibodies and exacerbate HO in FOP mice. This property is limited to FOP-mutant ACVR1, as WT ACVR1 is not activated by said antibodies. Given the catastrophic nature of HO in FOP, our results indicate that ACVR1 antibodies should not be considered as a therapeutic option in this condition. However, ACVR1 antibodies maybe offer of potential therapeutic option for trauma-induced HO in non-FOP settings and could also be considered in conditions where increasing iron levels is desirable.

Materials and Methods

Reagents

Activin A (338-AC-500/CF), BMP2 (355-BM-100/CF), BMP7 (354-BP-010/CF), BMP10 (2926-BP-025/CF), and ACVR1B-Fc (808-AR-100) were purchased from R&D systems. ACVR1 Fabs were generated from corresponding ACVR1 Mabs and purified in-house. Human ACVR1 (REGN3111) and mouse ACVR1 (REGN3407) ecto (amino acid 21-123).mmh (used in the binding experiments) were expressed and purified in-house. Activin A antibodies (REGN2476 and REGN2477), ACVR2A/B antibody, myc antibody (REGN642, used in the binding experiments), and hIgG4 isotype control antibody were expressed and purified in-house. ALK3 ecto (amino acid 24-152)-Fc and ACVR2B ecto (amino acid 23-133)-Fc soluble proteins were made in-house.

Antibody discovery and optimization

Human antibodies against ACVR1 (human and mouse cross-reactive) were isolated from a full-length human IgG synthetic naïve library using an *in vitro* yeast selection system and associated methods (13). An antibody library of approximately 10^{10} in diversity, was designed and propagated as described previously (13, 28). ACVR1-binding antibodies were enriched by incubation of biotinylated ACVR1-Fc and Myc-His monomeric ACVR1 at different concentrations with antibody expressing yeast cells followed by magnetic bead selection (Miltenyi Biotec) or flow cytometry on an Aria II cell sorter (BD Biosciences) using fluorescent streptavidin or extravidin secondary reagents in several successive selection rounds. Antibodies cross-reactive to off-target proteins ALK1, ALK3, and ALK6 were actively depleted from selection outputs. After the last round of enrichment, yeast cells were plated onto agar plates, analyzed by DNA sequencing, and expanded for IgG production. Heavy chains from the naïve outputs were used to prepare light chain diversification libraries, which were then used for additional selection rounds. In particular, heavy chains were extracted from the fourth naïve selection round outputs and transformed into a light chain library comprising 10^6 unique light chains to create new libraries approximately 10^8 in total diversity. Antibody optimization was completed in three phases. Optimization of the heavy chain via diversification of the complementarity-determining regions (CDRs) CDR-H1 and CDR-H2 followed either by mutagenic PCR-based diversification of the entire heavy chain variable region or diversification of the light chain CDR-L1 and CDR-L2 segments. CDR-H1 and CDR-H2 regions were diversified with premade libraries of CDR-H1 and CDR-H2 variants of a diversity of approximately 10^8. Mutagenic PCR-based and premade libraries with CDR-L1 and CDR-L2 variants had diversities of approximately 10^7 and 10^5, respectively. Lead variants were further diversified via DNA oligonucleotide sequence variegation of the CDR-H3 or CDR-L3. Oligonucleotide CDR-H3 and CDR-L3 libraries had a

diversity of approximately 10^4 and 10^3, respectively. Diversified antibody lineage populations were selected for enhanced binding to the target proteins while avoiding undesired cross-reactivity. The methods used for selections on diversified populations are similar or identical to those used to isolate the original lead IgGs (28). An additional ACVR1 antibody that recognizes only human ACVR1 was also used in this study and has been previously described (15).

FOP mouse model

Acvr1$^{[R206H]FlEx/+}$ (Acvr1$^{tm2.1Vlcg}$) and the accompanying Cre transgenic line, *GT(ROSA26)Sor*$^{CreERT2/+}$ (Gt(ROSA)26Sor$^{tm3.1(cre/ERT2)Vlcg}$), used to generate *Acvr1*$^{[R206H]FlEx/+}$*; GT(ROSA26)Sor*$^{CreERT2/+}$ mice have been previously described (7, 29). These were maintained in heterozygosity on a mixed C57BL/6NTac-129S6/SvEvTac background. All experiments were performed in accordance with the Institutional Animal Care and Use Committee of Regeneron. Both male and female mice were used between 8 and 27 weeks of age, however mice were age- and sex-matched between groups. The model was initiated by inversion of the R206H-encoding exon into the sense strand, which is accomplished by treating *Acvr1*$^{[R20H6]FlEx/+}$; *Gt(ROSA26)Sor*$^{CreERT2/+}$ mice with 40 mg/kg of tamoxifen (Sigma) in oil intraperitoneally (i.p.) daily for 5 days (to activate CreER^{T2}). HO was initiated by pinch injury to the gastrocnemius muscle using a hemostat for 15 seconds. To assess HO, mice were anesthetized by isofluorane and whole body-scanned, with a field of view at 60mm x120mm, using *in vivo* µCT (Quantum FX, PerkinElmer, Hopkinton, MA, USA). The X-ray source was set to a current of 160 µA, voltage of 90 kVp, with a voxel size at 120 or 240µm.

Antibody dosing of mice

For treatment studies mice were separated to ensure age and sex matching across groups, treatments were initiated on the same day as tamoxifen administration. Antibodies to ACVR1 (Mab 1, Mab 2 and Mab 3), Activin A (REGN2477, REGN2476) and an hIgG4 isotype control were used in these studies. Mice were injected subcutaneously (s.c.) with 10 mg/kg of antibodies twice weekly for the duration of the studies. Heterotopic bone lesions were visualized by *in vivo* µCT imaging.

Hydrodynamic delivery of ACVR1 Fabs

ACVR1 Fabs were delivered by hydrodynamic delivery (HDD) (30) 5 days post initiation of the model by tamoxifen. Briefly, 25 µg of DNA plasmid encoding the CH1 and VH domain and 25 µg of DNA plasmid encoding the CL and VL domains under the control of the ubiquitin promoter were diluted in 2 ml of PBS and injected in the tail vein in 5 to 7 seconds. HO was initiated in

the hindlimb by muscle pinch 7 days post HDD. Serum Fab concentration was measured 7 days post HDD by ELISA using a goat anti-kappa light chain antibody (ThermoFisher Scientific).

Serum hepcidin and iron measurements

Serum hepcidin was measured using a murine hepcidin ELISA kit (Intrinsic Biosciences) following the manufacturer's protocol. Serum iron was measured using the QuantiChrom Iron Assay Kit (BioAssay Systems, DIFE-250) following the manufacturer's protocol.

Fibro/adipogenic progenitor isolation and culture

Details of skeletal muscle dissection have been previously described (12). In brief, muscle was dissected *Acvr1*$^{[R206H]FlEx/+}$*; Gt(ROSA26)Sor*$^{CreERT2/+}$ mice and dissociated using the Skeletal Muscle Dissociation Kit (Miltenyi Biotec) and gentleMACS Octo Dissociator with heaters (Miltenyi Biotec), in accordance with manufacturer instructions. Following centrifugation at 300 g for 10 min at 4°C, the supernatant was discarded, and the pellet was resuspended in growth media (Dulbecco's Modified Eagle Medium (DMEM; Life Technologies) with 50 U/mL Penicillin and 50 µg/mL Streptomycin (Gibco) and 16.6% fetal bovine serum (FBS; Lot# 192K18, Avantor). Cells were then plated onto tissue culture flasks (Corning). Fluorescence assisted cell sorting (FACS) was performed on single cells incubated with anti-mouse PDGFRA APC (clone APA5, eBioscience) to label FAPs, as previously described (12, 31). FACS-isolated FAPs were seeded at a density of 2000 cells/cm2 onto tissue culture flasks (Corning) in growth media and maintained at 37°C in a humidified atmosphere at 5% CO2. Media was changed every other day. Prior to use, FAPs were treated with 2 µM (*Z*)−4-hydroxytamoxifen (Sigma-Aldrich) for 48 hours to induce inversion of the R206H-containing exon. All experiments were conducted with FAPs passaged fewer than 3 times.

Burn/tenotomy model of tHO

Wildtype C57/Bl6 mice were obtained from Taconic. The burn/tenotomy extremity-polytrauma model was performed as previously described (14, 15). Briefly, all mice received presurgical analgesia consisting of 0.06 mg·kg−1 buprenorphine for 48 hours, followed by anesthesia with inhaled isoflurane, and close postoperative monitoring with analgesic administration. Mice received 30% total body surface area partial thickness burn on a shaved dorsum followed by transection of the left Achilles tendon. Dorsal burn was induced using a metal block heated to 60 °C in a water bath and applied to the dorsum for 18 s continuously. Heterotopic bone was quantified by µCT by 5 weeks post-surgery.

Generation of type II receptor knockout mouse embryonic stem cells

Mouse embryonic stem cell (mESC) lines ablated for *Acvr2a, Acvr2b*, and/or *Bmpr2* were generated as follows. Briefly, CRISPR guides targeting the 5' and 3' ends of *Acvr2a* coding sequence were electroporated into a mouse ESC line harboring the tamoxifen inducible, conditional-on *Acvr1* R206H FOP allele ($Acvr1^{[R206H]FlEx/+}$; $Gt(ROSA26)Sor^{CreERT2/+}$) (7). ESC clones with biallelic collapses for *Acvr2a* were identified by TaqMan analysis and then electroporated with CRISPR guides to biallelically ablate *Acvr2b*, generating the cell line $Acvr2a^{-/-}$; $Acvr2b^{-/-}$; $Acvr1^{[R206H]FlEx}$; $Gt(ROSA26)Sor^{CreERT2/+}$. An $Acvr2a^{-/-}$; $Acvr2b^{-/-}$; $Bmpr2^{-/-}$; $Acvr1^{[R206H]FlEx}$; $Gt(ROSA26)Sor^{CreERT2/+}$ mESC line was generated in a similar manner, as was a $Bmpr2^{-/-}$; $Acvr1^{[R206H]FlEx}$; $Gt(ROSA26)Sor^{CreERT2/+}$ mESC line. All ESC lines were then expanded for further experimentation.

Culturing mouse embryonic stem cells and immunoblotting

Mouse embryonic stem (mES) cell lines were cultured on irradiated MEF puromycin-resistant feeders (Thermofisher, A34965) on gelatin-coated plates in complete KO-ES media (KO DMEM) (Gibco, 10829018) media containing 15% (v/v) ES-screened FBS, 2 mM L-Glutamine, penicillin/streptomycin (50 U/ml), 0.2% (v/v) beta-mercaptoethanol, 2 U/ml Leukemia Inhibitory Factor (MiliPore, ESG1107) at 37°C in a humidified atmosphere at 5% CO_2. The feeder cells were removed using magnetic feeder removal microbeads (Miltenyi Biotech, 130-095-531) by following the manufacturer's protocol. Approximately 300,000 mES cells/well were plated in a 24-well gelatin-coated plate. After 24 hours of growing in 2i media (32), mES cells were treated with 100 nM Tamoxifen in 2i media for 24 hours to induce inversion of FOP mutant ACVR1 (7). On the following day, mES cells were switched to serum-free media for 2 hours before 1 hour treatment with various ligands, Mabs or Fabs. Subsequently, cells were lysed in RIPA buffer (Thermofisher, 89900) containing 2X protease and phosphatase inhibitors (Thermofisher, 78441). Total protein concentration was determined by BCA kit (Thermofisher, 23227). Equal amounts of protein (10 µg) were separated under reducing conditions on 4–12% Novex WedgeWell gels (Invitrogen) and transferred to PVDF membranes (Advansta). Membranes were blocked with Superblock (Thermofisher, 37536) for 3 hours at room temperature and incubated with primary antibodies from Cell Signaling Technology at a 1:1000 dilution (anti-phospho-Smad1/5/8 (41D10)), or 1:5000 (anti-β-actin (8H10D10)) overnight at 4°C, followed by incubation with horseradish peroxidase-conjugated secondary antibody at a 1:5000 dilution (7074) for 3 hours at room temperature. Western Bright ECL HRP substrate was used for detection (Advansta, K-12045-D20). A minimum of two independent biological replicates were performed for each experimental condition.

Immunoprecipitation

W20 (mouse bone stromal cells) cells and Hek293 (human embryonic kidney cells) cells were grown in Dulbecco's modified Eagle's medium containing 10% (v/v) fetal bovine serum (FBS), penicillin/streptomycin (50 U/ml), and 2 mM L-glutamine. These cells were transfected with Myc-ACVR1, Myc-ACVR1[R206H], and HA-ACVRIIB alone or in various combinations. W20 cells were transfected using X-tremeGENE 9 DNA transfection reagent (Sigma-Aldrich, 06 365 787 001) and Hek293 cells were transfected using TransIT-293 DNA transfection (MirusBio, MIR 2700) by following manufacturers' protocols. After transfections, cells were incubated overnight in the complete media. The following day, cells were switched to serum-free media (in the presence or absence of ACVRIIB-Fc). 48 hours after transfection, membrane fractions of the transfected cells were isolated using the Mem-PER Plus membrane protein extraction kit (Thermofisher, 89842). Membrane fractions were resuspended in the lysis buffer of the myc-IP kit (Thermofisher, 88844) and myc immunoprecipitation (IP) was performed using isolated membrane fractions by following the manufacturer's protocol. Immunoblotting was performed using IP input and elution samples as described above. ACVR1 antibody (Abcam, ab155981) and HA antibody (Cell Signaling, 3724) were used detect Myc-ACVR1 and HA-ACVRIIB, respectively.

Reporter gene assay

Hek293/BRE (Smad1/5/8 responsive)-Luc stable pools of reporter cells were generated. Reporter gene assay was performed as previously described (7). Briefly, ~ 10,000 cells/well were plated in a 96-well plate in complete media. After 16 hours incubation with ligands alone or in the presence of ACVR1 Mabs and Fabs, luciferase expression was measured using the Bright-Glo luciferase assay system (Promega, E2650).

DmrB homodimerization assay

Hek293/BRE-Luc stable cells were transfected with hACVR1-DmrB or hACVR1[R206H]-DmrB vectors. High ACVR1 expressing cells were isolated with FACS (fluorescence activated cell sorting) as previously described (7). Approximately 10,000 cells/well were plated in a 96-well plate in the complete media. After 16 hours of incubation with B/B homodimerizer (Takara Bio, 635059) at various concentrations, luciferase expression was measured using the Bright-Glo luciferase assay system. In order to confirm the activity of the generated DmrB cell lines, Hek293.BRE.hACVR1-DmrB and Hek293.BRE.hACVR1[R206H]-DmrB cells were treated with 20 nM B/B homodimerizer for 16 hours in the serum-free media. The following day, these cells were treated with various concentrations of Activin A or BMP7 in the 20 nM B/B

homodimerizer containing serum-free media. 16 hours after the ligand treatment, luciferase expression was measured using the Bright-Glo luciferase assay system.

Surface expression of ACVR1

Acvr1$^{[R206H]/+}$ *and Acvr2a* $^{-/-}$*;Acvr2b* $^{-/-}$*;Bmpr2* $^{-/-}$*;Acvr1*$^{[R206H]/+}$ mES cells were dissociated using non-enzymatic cell dissociation buffer (MiliPore, S-004-B) and resuspended in the flow cytometry staining buffer (R&D systems, FC001). After 15 minutes of blocking (Thermofisher, 14-9161-73), cells were stained with ACVR1 primary antibody (R&D systems, MAB637) for 1 hour followed by staining with Alexa 647 secondary antibody (Thermofisher, A-21236) for 30 minutes. Stained cells were fixed with CytoFix (BD Biosciences, 554655) and passed through a filter block (Pall, PN 8027). All the steps were carried out in the flow cytometry staining buffer at dark on ice. Stained cells were analyzed using CytoFLEX (Beckman) instrument.

Binding kinetics measurements

Kinetic binding parameters for the interaction of ACVR1 Mabs and Fabs with human and mouse ACVR1 were determined on Biacore T200 using dextran-coated (CM5) chips at 37 °C. The running buffer was prepared using filtered HBS-EP (10 mM Hepes, 150 mM NaCl, 3.4mM EDTA, 0.05% polysorbate 20, pH 7.4). In order to measure ACVR1 Mab interactions with human and mouse ACVR1, an anti-hFc antibody was immobilized on a CM5 chip as previously described (8). After capturing ~ 250 RU (response units) of ACVR1 Mabs, hACVR1.mmh and mACVR1.mmh were injected over ACVR1 Mabs at 50 µL/min for 90 seconds followed by 20 minutes dissociation. In order to measure ACVR1 Fab interactions with human and mouse ACVR1, an anti-myc antibody was immobilized on a CM5 chip. After capturing equal response units of a mouse or human ACVR1.mmh on the surface, ACVR1 Fabs were injected at 50 µL/min for 90 seconds followed by 20 minutes dissociation. Kinetic parameters were obtained by globally fitting the real-time binding data to a 1:1 Langmuir binding model using Scrubber 2.0c Evaluation Software. The equilibrium dissociation constant (K_D) was calculated by dividing the dissociation rate constant (k_d) by the association rate constant (k_a).

Author contributions

SJH, VI, and ANE designed the study, and analyzed data. SA, LH, LW, ND, SR, YR, QZ, NR, KCN, VK, SB, LC, JLS, and KS carried out the experiments and analyzed data. SJH, VI, ANE, PBY, AJM, SA, and LJ wrote the manuscript, which was reviewed by all authors. SA and LW contributed equally to the manuscript; assignment of order of authorship was alphabetical and based on their last names.

Acknowledgements

The authors thank the following contributors for providing support: VelociGene team for generating the ES cells and mice used in this study and the vivarium staff for animal husbandry; members of the departments of Therapeutic Proteins, Protein Expression Sciences, and Preclinical Manufacturing and Process Development for immunization and production of antibodies, stable cell lines, and large-scale production of proteins; members of the DNA Core and Molecular Profiling for plasmid production and RNAseq analysis; Jen Symonds and Tyler Billipp (Adimab) for help with antibody discovery and optimization.

References

1. Pignolo RJ, Baujat G, Brown MA, De Cunto C, Di Rocco M, Hsiao EC, et al. Natural history of fibrodysplasia ossificans progressiva: cross-sectional analysis of annotated baseline phenotypes. *Orphanet J Rare Dis.* 2019;14(1):98.
2. Shore EM, Xu M, Feldman GJ, Fenstermacher DA, Cho TJ, Choi IH, et al. A recurrent mutation in the BMP type I receptor ACVR1 causes inherited and sporadic fibrodysplasia ossificans progressiva. *Nat Genet.* 2006;38(5):525-7.
3. Petrie KA, Lee WH, Bullock AN, Pointon JJ, Smith R, Russell RG, et al. Novel mutations in ACVR1 result in atypical features in two fibrodysplasia ossificans progressiva patients. *PLoS One.* 2009;4(3):e5005.
4. Huning I, and Gillessen-Kaesbach G. Fibrodysplasia ossificans progressiva: clinical course, genetic mutations and genotype-phenotype correlation. *Molecular syndromology.* 2014;5(5):201-11.
5. Kaplan FS, Chakkalakal SA, and Shore EM. Fibrodysplasia ossificans progressiva: mechanisms and models of skeletal metamorphosis. *Dis Model Mech.* 2012;5(6):756-62.
6. Gorter DJJ, S·nchez-Duffhues G, and Dijke P. Promiscuous signaling of ligands via mutant ALK2 in fibrodysplasia ossificans progressiva. *Receptors and clinical investigation.* 2016;3.
7. Hatsell SJ, Idone V, Wolken DM, Huang L, Kim HJ, Wang L, et al. ACVR1R206H receptor mutation causes fibrodysplasia ossificans progressiva by imparting responsiveness to activin A. *Science translational medicine.* 2015;7(303):303ra137.
8. Aykul S, Corpina RA, Goebel EJ, Cunanan CJ, Dimitriou A, Kim HJ, et al. Activin A forms a non-signaling complex with ACVR1 and type II Activin/BMP receptors via its finger 2 tip loop. *Elife.* 2020;9.
9. Upadhyay J, Xie L, Huang L, Das N, Stewart RC, Lyon MC, et al. The Expansion of Heterotopic Bone in Fibrodysplasia Ossificans Progressiva Is Activin A-Dependent. *J Bone Miner Res.* 2017;32(12):2489-99.
10. Hino K, Ikeya M, Horigome K, Matsumoto Y, Ebise H, Nishio M, et al. Neofunction of ACVR1 in fibrodysplasia ossificans progressiva. *Proc Natl Acad Sci U S A.* 2015;112(50):15438-43.

11. Dey D, Bagarova J, Hatsell SJ, Armstrong KA, Huang L, Ermann J, et al. Two tissue-resident progenitor lineages drive distinct phenotypes of heterotopic ossification. *Science translational medicine.* 2016;8(366):366ra163-366ra163.
12. Lees-Shepard JB, Yamamoto M, Biswas AA, Stoessel SJ, Nicholas SE, Cogswell CA, et al. Activin-dependent signaling in fibro/adipogenic progenitors causes fibrodysplasia ossificans progressiva. *Nat Commun.* 2018;9(1):471.
13. Rouha H, Badarau A, Visram ZC, Battles MB, Prinz B, Magyarics Z, et al. Five birds, one stone: neutralization of alpha-hemolysin and 4 bi-component leukocidins of Staphylococcus aureus with a single human monoclonal antibody. *MAbs.* 2015;7(1):243-54.
14. Peterson JR, De La Rosa S, Sun H, Eboda O, Cilwa KE, Donneys A, et al. Burn injury enhances bone formation in heterotopic ossification model. *Ann Surg.* 2014;259(5):993-8.
15. Hwang C, Pagani CA, Das N, Marini S, Huber AK, Xie L, et al. Activin A does not drive post-traumatic heterotopic ossification. *Bone.* 2020;138:115473.
16. Steinbicker AU, Bartnikas TB, Lohmeyer LK, Leyton P, Mayeur C, Kao SM, et al. Perturbation of hepcidin expression by BMP type I receptor deletion induces iron overload in mice. *Blood.* 2011;118(15):4224-30.
17. Andriopoulos B, Jr., Corradini E, Xia Y, Faasse SA, Chen S, Grgurevic L, et al. BMP6 is a key endogenous regulator of hepcidin expression and iron metabolism. *Nat Genet.* 2009;41(4):482-7.
18. Meynard D, Kautz L, Darnaud V, Canonne-Hergaux F, Coppin H, and Roth MP. Lack of the bone morphogenetic protein BMP6 induces massive iron overload. *Nat Genet.* 2009;41(4):478-81.
19. Kaplan FS, Kobori JA, Orellana C, Calvo I, Rosello M, Martinez F, et al. Multi-system involvement in a severe variant of fibrodysplasia ossificans progressiva (ACVR1 c.772G>A; R258G): A report of two patients. *Am J Med Genet A.* 2015;167A(10):2265-71.
20. Clackson T, Yang W, Rozamus LW, Hatada M, Amara JF, Rollins CT, et al. Redesigning an FKBP-ligand interface to generate chemical dimerizers with novel specificity. *Proc Natl Acad Sci U S A.* 1998;95(18):10437-42.
21. Le VQ, and Wharton KA. Hyperactive BMP signaling induced by ALK2(R206H) requires type II receptor function in a Drosophila model for classic fibrodysplasia ossificans progressiva. *Dev Dyn.* 2012;241(1):200-14.
22. Bagarova J, Vonner AJ, Armstrong KA, Borgermann J, Lai CS, Deng DY, et al. Constitutively active ALK2 receptor mutants require type II receptor cooperation. *Mol Cell Biol.* 2013;33(12):2413-24.
23. Ramachandran A, Mehic M, Wasim L, Malinova D, Gori I, Blaszczyk BK, et al. Pathogenic ACVR1(R206H) activation by Activin A-induced receptor clustering and autophosphorylation. *EMBO J.* 2021:e106317.
24. Ehrlich M, Horbelt D, Marom B, Knaus P, and Henis YI. Homomeric and heteromeric complexes among TGF-beta and BMP receptors and their roles in signaling. *Cell Signal.* 2011;23(9):1424-32.

25. Katagiri T, Tsuji S, Tsukamoto S, Kuratani M, Ohte S, Takaishi K, et al. An antibody against ALK2 extracellular domain reveals a role of dimer formation for signal activation. *Journal of Bone and Mineral Research.* 2018;33(S1):S1-S464.
26. Yaden BC, Wang YX, Wilson JM, Culver AE, Milner A, Datta-Mannan A, et al. Inhibition of activin A ameliorates skeletal muscle injury and rescues contractile properties by inducing efficient remodeling in female mice. *Am J Pathol.* 2014;184(4):1152-66.
27. Fukuda T, Scott G, Komatsu Y, Araya R, Kawano M, Ray MK, et al. Generation of a mouse with conditionally activated signaling through the BMP receptor, ALK2. *Genesis.* 2006;44(4):159-67.
28. Xu Y, Roach W, Sun T, Jain T, Prinz B, Yu TY, et al. Addressing polyspecificity of antibodies selected from an in vitro yeast presentation system: a FACS-based, high-throughput selection and analytical tool. *Protein Eng Des Sel.* 2013;26(10):663-70.
29. Economides AN, Frendewey D, Yang P, Dominguez MG, Dore AT, Lobov IB, et al. Conditionals by inversion provide a universal method for the generation of conditional alleles. *Proc Natl Acad Sci U S A.* 2013;110(34):E3179-88.
30. Liu F, Song Y, and Liu D. Hydrodynamics-based transfection in animals by systemic administration of plasmid DNA. *Gene Ther.* 1999;6(7):1258-66.
31. Lees-Shepard JB, Nicholas SE, Stoessel SJ, Devarakonda PM, Schneider MJ, Yamamoto M, et al. Palovarotene reduces heterotopic ossification in juvenile FOP mice but exhibits pronounced skeletal toxicity. *Elife.* 2018;7.
32. Tamm C, Pijuan Galito S, and Anneren C. A comparative study of protocols for mouse embryonic stem cell culturing. *PLoS One.* 2013;8(12):e81156.

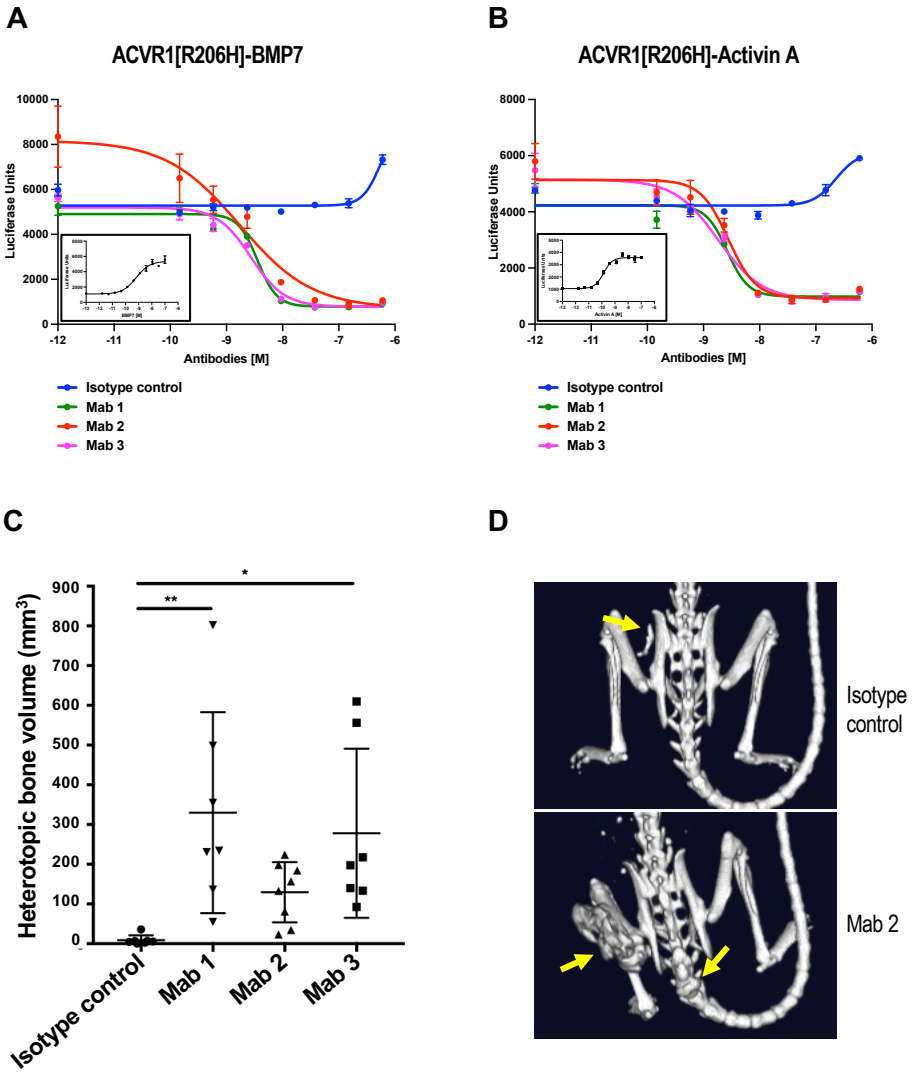

Figure 1: ACVR1 antibodies block BMP7 and Activin A signaling in Hek293.ACVR1[R206H] cells but increase heterotopic bone formation in FOP mice.

Stable pools of Hek293/BRE-Luc reporter cells overexpressing ACVR1[R206H] were treated with 2 nM BMP7 (**A**) or 2 nM Activin A (**B**). ACVR1 antibodies inhibited Smad1/5/8 phosphorylation induced by BMP7 or Activin A (**A-B**). Inserts in panel A and B show the dose response of BMP7 and Activin A respectively, on Hek293/BRE-Luc reporter cells overexpressing ACVR1[R206H]. (**C**) *Acvr1*$^{[R206H]FlEx/+}$; *GT(ROSA26)Sor*$^{CreERT2/+}$ mice were injected with tamoxifen to initiate the model and concurrently injected with ACVR1 antibodies or isotype control antibody at 10 mg/kg weekly (n=7-8/group). Total heterotopic bone lesion volume was measured at 4 weeks post initiation. Data show the mean ± SD, *p<0.05, **p<0.01; 1 way ANOVA with Dunnett's multiple-comparison test. (**D**) Representative µCT images of FOP mice (*Acvr1*$^{[R206H]FlEx/+}$; *GT(ROSA26)Sor*$^{CreERT2/+}$ post-tamoxifen) treated with ACVR1 antibody or isotype control antibody. Yellow arrows indicate the positions of heterotopic bone lesions.

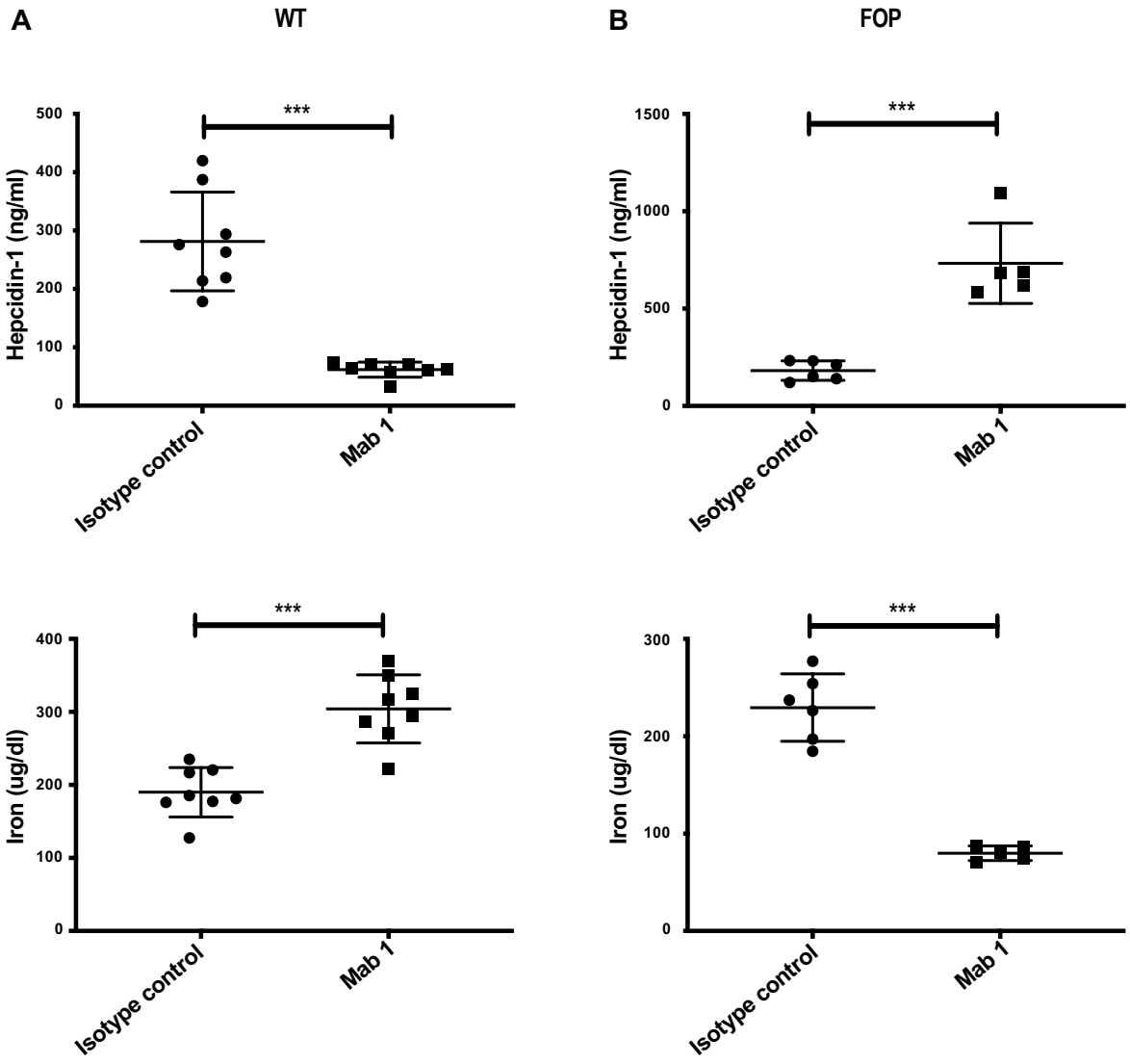

Figure 2: ACVR1 antibody-induced changes in Hepcidin and iron levels are consistent with inhibition of WT ACVR1 and activation of ACVR1[R206H] *in vivo*.
(**A**) In WT mice (n=8/group) ACVR1 Mab 1 decreased serum Hepcidin and increased serum iron. **(B)** In FOP mice (*Acvr1*$^{[R206H]FlEx/+}$; *GT(ROSA26)Sor*$^{CreERT2/+}$ post-tamoxifen) (n=5-6/group) ACVR1 Mab 1 increased serum hepcidin and decreased serum iron. *** $p<0.001$ t-test

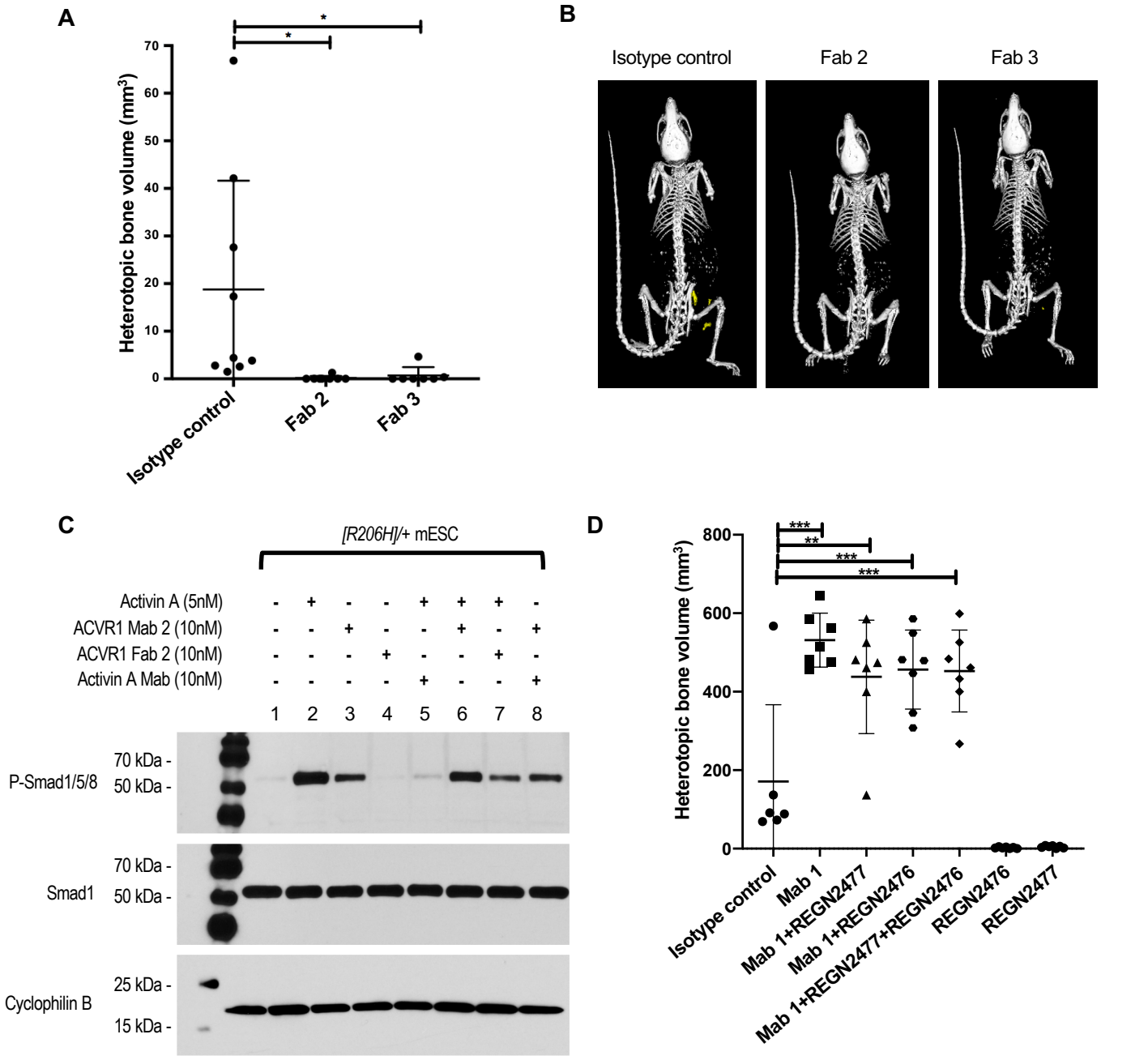

Figure 3: Dimeric ACVR1 antibodies activate whereas monomeric ACVR1 Fabs block ACVR1[R206H]. (**A**) *Acvr1*$^{[R206H]FlEx/+}$*; GT(ROSA26)Sor*$^{CreERT2/+}$ mice received plasmids expressing ACVR1 Fabs or a plasmid encoding a control Mab by HDD 5 days after initiation of the model with tamoxifen. HO was triggered in the hindlimb by muscle pinch 7 days post HDD and total heterotopic bone volume was measured at 4 weeks post injury. FOP mice (*Acvr1*$^{[R206H]FlEx/+}$*; GT(ROSA26)Sor*$^{CreERT2/+}$ post-tamoxifen) expressing ACVR1 Fab showed reduced HO compared to control mice. Data show the mean ± SD, *p<0.05, 1 way ANOVA with Dunnett's multiple-comparison test. (**B**) Representative µCT images of FOP mice expressing either ACVR1 Fab or an isotype control antibody. (**C**) *Acvr1*$^{[R206H]/+}$*; GT(ROSA26)Sor*$^{CreERT2/+}$ (*[R206H]/+*) mouse ES cells were treated with Activin A, ACVR1 Mab 2, ACVR1 Fab 2 or Activin A Mab (REGN2476) in various combinations for 1 hour. Activin A and ACVR1 Mab 2 but not ACVR1 Fab 2 induced Smad1/5/8 phosphorylation. ACVR1 Fab 2 significantly reduced Activin A induced Smad1/5/8 phosphorylation, whereas ACVR1 Mab 2 only slightly reduced Activin A induced Smad1/5/8 phosphorylation. (**D**) ACVR1 antibody activation of ACVR1[R206H] is independent of Activin A. *Acvr1*$^{[R206H]FlEx/+}$*; GT(ROSA26)Sor*$^{CreERT2/+}$ mice (n=6-8/group) were injected with tamoxifen to initiate the model and concurrently injected with antibodies at 10 mg/kg weekly. Total heterotopic bone volume was measured at 3 weeks post initiation. Data show the mean ± SD, **p<0.01, ***p<0.001; 1 way ANOVA with Dunnett's multiple-comparison test.

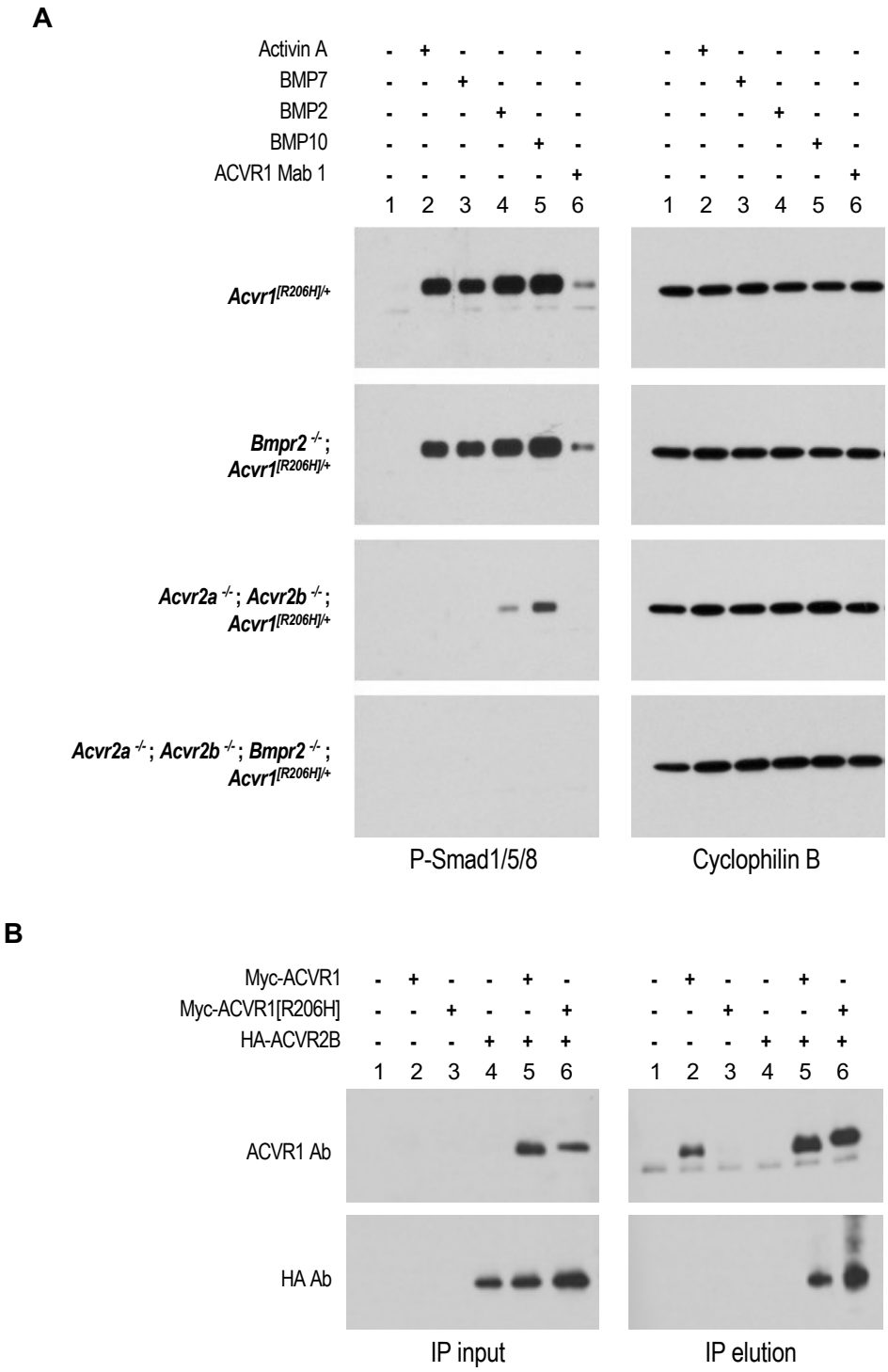

Figure 4: ACVR1 antibody activation of ACVR1[R206H] is type II receptor dependent.
(**A**) *Acvr1*$^{[R206H]/+}$*; GT(ROSA26)Sor*$^{CreERT2/+}$ (*[R206H]/+*) mouse ES cells lacking *Acvr2a* plus *Acvr2b,* or *Bmpr2* or all three of these type II receptor genes were treated with 10 nM Activin A, BMP7, BMP2, BMP10 or ACVR1 Mab 1 for 1 hour. Activin A, BMP7, BMP2, BMP10 and ACVR1 Mab 1 induced Smad1/5/8 phosphorylation in cells that lack *Bmpr2* but retain *Acvr2a* and *Acvr2b*, but not in cells where *Acvr2a* and *Acvr2b* or all three type II receptors have been knocked out. (**B**) ACVR2B co-immunoprecipitates with both ACVR1 and ACVR1[R206H] from W20 cells expressing Myc-tagged ACVR1 and/or HA-tagged ACVR2B. Myc-ACVR1 was immunoprecipitated using a Myc antibody. ACVR1 and ACVR2B were detected using an ACVR1 or HA antibody, respectively.

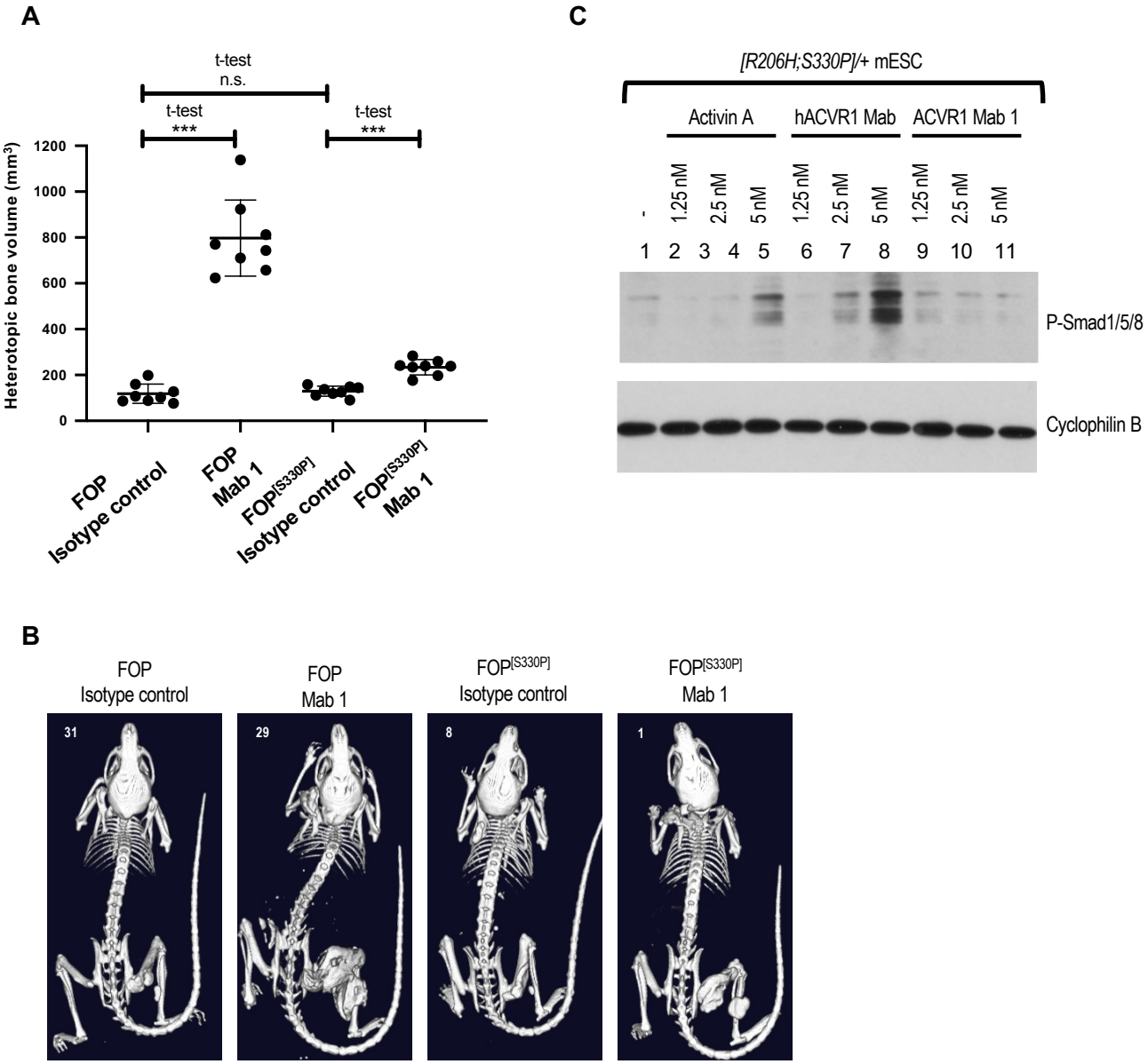

Figure 5: ACVR1[R206H;S330P] is activated by ACVR1 antibodies but to a lesser degree than ACVR1[R206H].

(**A**, **B**) *Acvr1*$^{[R206H]FlEx/+}$; *GT(ROSA26)Sor*$^{CreERT2/+}$ mice or *Acvr1*$^{huecto;[R206H]FlEx;[S330P]/+}$; *GT(ROSA26)Sor*$^{CreERT2/+}$ (*FOP*$^{[S330P]}$) mice were injected with tamoxifen to initiate the model and concurrently injected with ACVR1 Mab 1 or isotype control antibody at 10 mg/kg weekly (n=8/group). Total heterotopic bone volume was measured 3 weeks post initiation of the model. ACVR1 Mab 1 increased HO compared to isotype control in both mouse models though to a lesser degree in *FOP*$^{[S330P]}$ mice. Data show the mean ± SD, ***p<0.001; t-test. (**C**) *Acvr1*$^{huecto;[R206H;S330P]/+}$; *GT(ROSA26)Sor*$^{CreERT2/+}$ (*[R206H;S330P]/+*) mouse ES cells were treated with 10 nM Activin A, ACVR1 Mab 1 or hACVR1 antibody and assessed for phospho Smad1/5/8. hACVR1 Mab (that only binds ACVR1[huecto;R206H;S330P] and not WT mouse ACVR1) induced Smad1/5/8 phosphorylation, whereas Mab 1 (which recognizes both human and mouse ACVR1) did not drive an appreciable level of Smad1/5/8 phosphorylation.

SUPPLEMENTAL FIGURES

Supplemental Table 1: Binding constants of ACVR1 Mabs and Fabs to human ACVR1

ACVR1 Mab Tested	k_a (1/Ms)	k_d (1/s)	K_D (M)	$t^{1/2}$ (min)
Mab 1	1.31E+06	1.59E-03	1.21E-09	7
Mab 2	7.18E+05	1.63E-04	2.27E-10	71
Mab 3	6.77E+05	1.76E-04	2.60E-10	65
Fab 2	5.49E+05	9.36E-05	1.70E-10	123
Fab 3	6.90E+05	1.06E-04	1.54E-10	109
hACVR1 Mab	2.30E+05	1.33E-03	5.80E-09	9

In order to measure the binding constants of ACVR1 Mabs, Mabs were captured with an anti-human Fc antibody immobilized on a CM5 chip. Different concentrations of hACVR1.mmh (REGN3111) were injected over ACVR1 Mabs at 37 ^{0}C. In order to measure the binding constants of ACVR1 Fabs, hACVR1.mmh was captured with a myc antibody (REGN642) immobilized on a CM5 chip. Different concentrations of ACVR1 Fabs were injected over hACVR1.mmh at 37 ^{0}C. Binding rate constants and equilibrium dissociation rate constants were calculated by fitting data using 1:1 Langmuir binding model (Scrubber 2.0c). All 3 ACVR1 Fabs bound to monomeric human ACVR1 with binding kinetics similar (< 2.5-fold difference) to their respective Mabs.

Supplemental Table 2: Binding constants of ACVR1 Mabs and Fabs to mouse ACVR1

ACVR1 Mab Tested	k_a (1/Ms)	k_d (1/s)	K_D (M)	$t^{1/2}$ (min)
Mab 1	1.34E+06	1.67E-03	1.24E-09	7
Mab 2	7.13E+05	1.61E-04	2.26E-10	72
Mab 3	6.74E+05	1.81E-04	2.68E-10	64
Fab 2	5.45E+05	9.72E-05	1.78E-10	119
Fab 3	6.53E+05	1.05E-04	1.60E-10	110
hACVR1 Mab	ND	ND	ND	ND

In order to measure the binding constants of ACVR1 Mabs, Mabs were captured with an anti-human Fc antibody immobilized on a CM5 chip. Different concentrations of mACVR1.mmh (REGN3407) were injected over ACVR1 Mabs at 37 ^{0}C. In order to measure the binding constants of ACVR1 Fabs, mACVR1.mmh was captured with a myc antibody (REGN642) immobilized on a CM5 chip. Different concentrations of ACVR1 Fabs were injected over mACVR1.mmh at 37 ^{0}C. Binding rate constants and equilibrium dissociation rate constants were calculated by fitting data using 1:1 Langmuir binding model (Scrubber 2.0c). All 3 ACVR1 Fabs bound to monomeric mouse ACVR1 with binding kinetics similar (< 2.5-fold difference) to their respective Mabs. hACVR1 Mab didn't bind mACVR1.mmh in the tested concentration range.

Supplemental Table 3: ACVR1 antibodies are specific to ACVR1

		100 nM Human Receptor Binding				100 nM Mouse Receptor Binding			
Mab Captured	**Mab Capture Level (RU)**	**ACVR1**	**ACVRL1**	**BMPR1A**	**BMPR1B**	**ACVR1**	**ACVRL1**	**BMPR1A**	**BMPR1B**
Mab 1	264 ± 4	147 ± 4	2 ± 0	2 ± 0.1	20 ± 0.6	140 ± 2.3	3 ± 0.4	8 ± 0.2	1 ± 0.2
Mab 2	261 ± 0.5	130 ± 0.4	1 ± 0.1	2 ± 0.1	10 ± 0.5	130 ± 1.5	1 ± 0.1	3 ± 0.1	1 ± 0.1
Mab 3	272 ± 2.2	147 ± 2.2	4 ± 0.1	2 ± 0	24 ± 0.6	141 ± 5.4	4 ± 0.4	9 ± 0.1	1 ± 0.1
hACVR1 Mab	251 ± 0.9	98 ± 1.4	0 ± 0.1	0 ± 0.1	3 ± 0.1	63 ± 1.5	0 ± 0.2	1 ± 0.1	0 ± 0.3
Isotype control	236 ± 0.8	11 ± 1.2	2 ± 0	1 ± 0.1	19 ± 0.5	8 ± 1	2 ± 0.2	7 ± 0.1	1 ± 0

In order to measure the specificity of ACVR1 Mabs, ACVR1 Mabs were captured with anti-human Fab immobilized on a CM5 chip. 100 nM or 10 nM of dimeric human or mouse ACVR1, ACVRL1, BMPR1A or BMPR1B were injected at 30 µL/min for 2 min (duplicate injections) and the experiment was performed at 25°C. Binding of different receptors to the captured Mab was determined using Scrubber 2.0c. None of the ACVR1 Mabs bound to any of the other receptors indicating that these Mabs are specific to ACVR1.

Supplemental Table 4: Cross-competition data of ACVR1 antibodies

2nd Mab / 1st Mab	hACVR 1 Mab	Mab 3	Mab 2	Mab 1	Isotype control
hACVR1 Mab	0.04	0.06	0.74	0.80	0.04
Mab 3	0.06	0.03	0.10	0.80	0.05
Mab 2	0.75	0.17	0.04	0.07	0.05
Mab 1	0.75	0.68	0.04	0.04	0.04
Isotype control	0.64	0.65	0.61	0.66	0.07

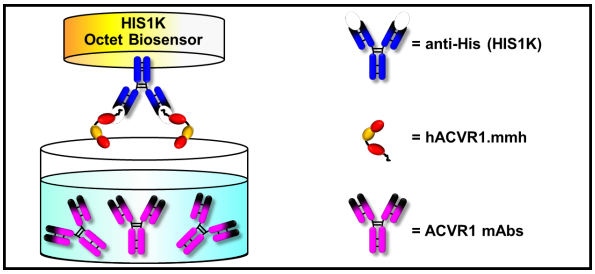

The hACVR1.mmh was captured on a His antibody Octet biosensor and were later saturated by dipping into wells containing 50 µg/mL of ACVR1 Mabs (referred to as 1st Mab) for 4 min. Then, 1st Mab saturated biosensors were dipped into the wells containing 50 µg/mL of different ACVR1 Mabs (referred to as 2nd Mab) for 3 min. The binding of 2nd Mab to the complex of hACVR1.mmh and 1st Mab was determined, and the observed wavelength shift (nm) is reported in the Table. Isotype control was used as a negative control. The cells highlighted in red represent bidirectional competition while white cells represent no competition. A schematic depiction of the experiment is shown below the table.

These data indicate that hACVR1 Mab likely shares an epitope with Mab 3; Mab 3 and Mab2 recognize partially overlapping epitopes (or, alternatively, that binding of one of them to ACVR1 sterically hinders the binding of the other); and that Mab 1 and Mab 2 likely bind overlapping epitopes. Note that there is no cross-competition between hACVR1 Mab and Mab 1 and there is also no cross-competition between Mab 1 and Mab 3, indicating that the epitope recognized by Mab 1 is distinct from that recognized by hACVR1 Mab and Mab 3. Although hACVR1 Mab and Mab 3 appear to recognize overlapping epitopes, their binding properties differ significantly, as hACVR1 recognizes only human ACVR1, whereas Mab 3 recognizes both mouse and human ACVR1 (data not shown). Lastly, there is also no cross-competition between hACVR1 and Mab 2.

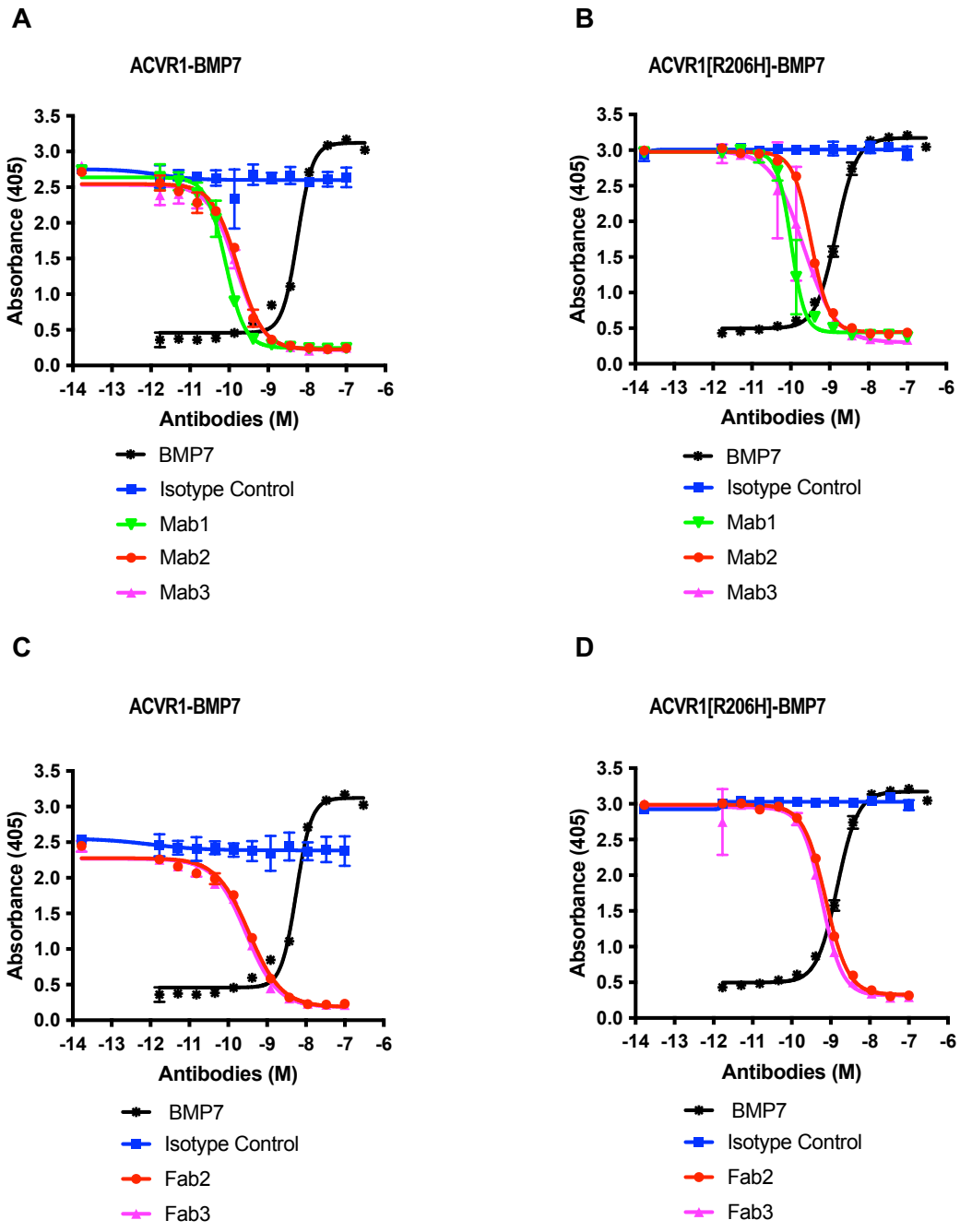

Supplemental Figure 1: Both ACVR1 antibodies and Fabs block BMP7 induced alkaline phosphatase activity.

Alkaline phosphatase activity was measured in W20s overexpressing either ACVR1 WT (**A**, **C**) or ACVR1[R206H] (**B**, **D**) treated with 10 nM BMP7. Both ACVR1 antibodies and ACVR1 Fabs showed inhibition of alkaline phosphatase activity induced by BMP7 in ACVR1 and ACVR1[R206H] overexpressing W20 cells.

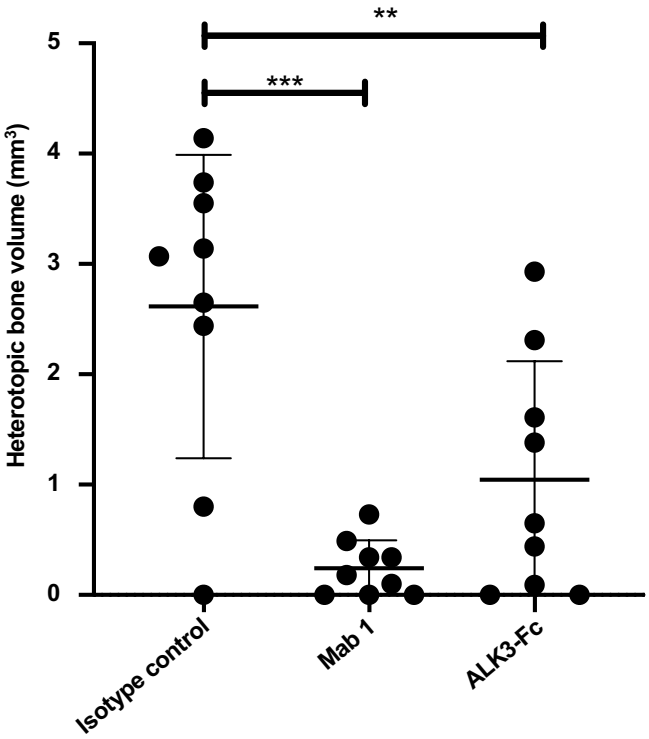

Supplemental Figure 2: ACVR1 antibodies reduce trauma-induced HO (tHO) in WT mice.
Mice (n=9/group) were administered either isotype control, ACVR1 Mab 1 or ALK3-Fc starting concurrently with induction of injury. Heterotopic bone volume was measured by µCT 5 weeks post injury. ACVR1 Mab 1 and ALK3-Fc significantly reduced heterotopic bone volume compared to isotype control treated mice. Data show the mean ± SD, **$p<0.01$, ***$p<0.001$; 1 way ANOVA with Dunnett's multiple-comparison test.

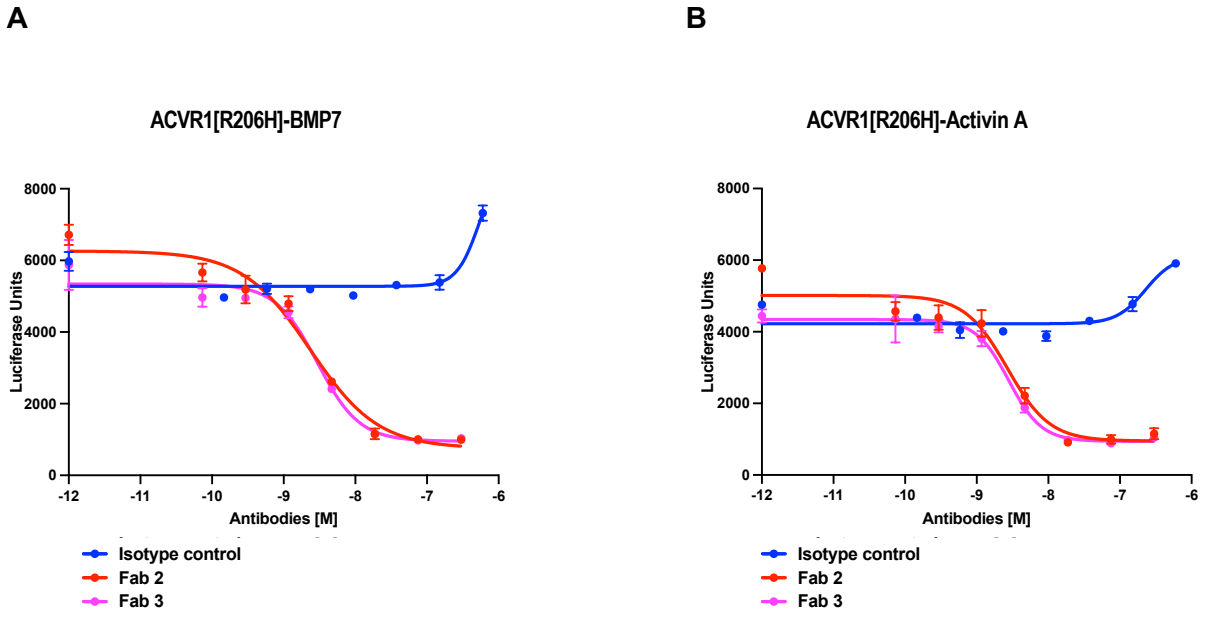

Supplemental Figure 3: ACVR1 Fabs block BMP7 and Activin A signaling in Hek293.ACVR1[R206H] cells.

Stable pools of Hek293/BRE-Luc reporter cells overexpressing ACVR1[R206H] were treated with 2 nM BMP7 (**A**) or 2 nM Activin A (**B**). ACVR1 Fabs inhibited Smad1/5/8 phosphorylation induced by BMP7 or Activin A.

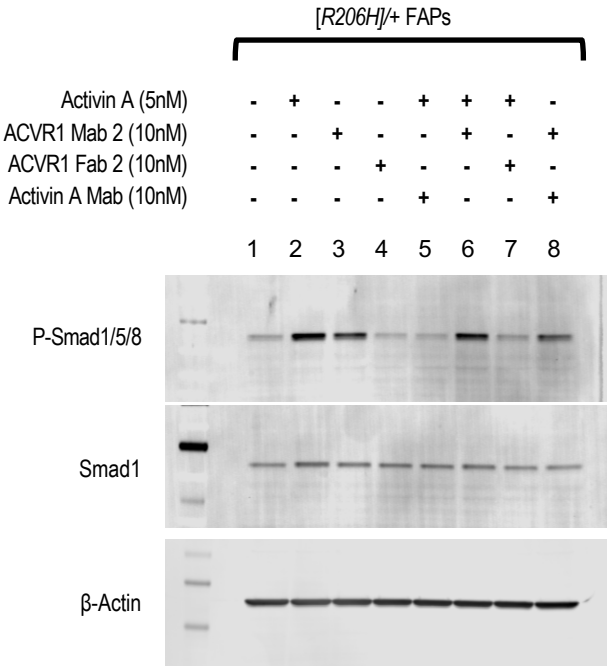

Supplemental Figure 4: ACVR1 antibodies activate whereas ACVR1 Fabs block ACVR1[R206H]. FAPs isolated from the FOP mice (*Acvr1*$^{[R206H]FlEx/+}$*; GT(ROSA26)Sor*$^{CreERT2/+}$ post tamoxifen*)* were treated with Activin A, ACVR1 Mab 2, ACVR1 Fab 2 or an Activin A neutralizing Mab (REGN2476) in various combinations for 1 hour. Activin A and ACVR1 Mab 2 but not ACVR1 Fab 2 induced Smad1/5/8 phosphorylation. ACVR1 Fab 2 blocked Activin A induced Smad1/5/8 phosphorylation to background levels, whereas the ACVR1 Mab 2 only partially blocks Activin A induced Smad1/5/8 phosphorylation. The Activin A Mab reduced baseline levels of Smad1/5/8 phosphorylation, and – as would be expected – blocked Activin A induced phosphorylation to background levels.

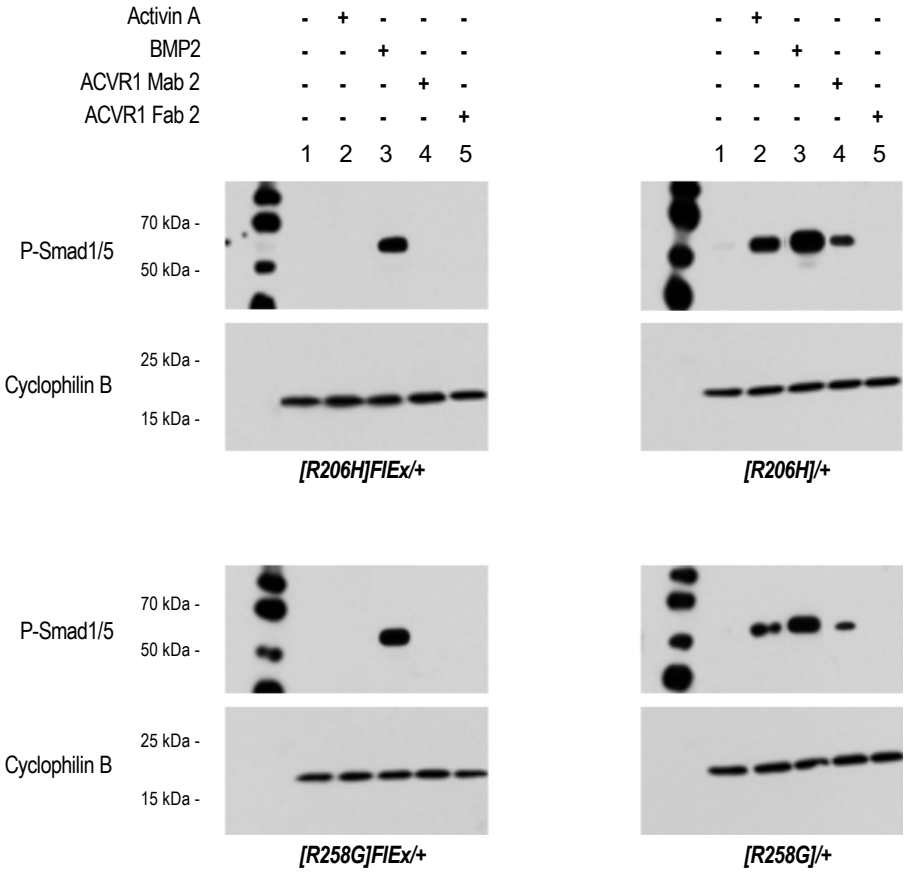

Supplemental Figure 5: ACVR1 antibodies activate both ACVR1[R206H] and ACVR1[258G], but not wild type ACVR1.
Acvr1$^{[R206H]FlEx/+}$*; GT(ROSA26)Sor*$^{CreERT2/+}$ (*[R206H]FlEx/+*) and *Acvr1*$^{[R258G]FlEx/+}$*; GT(ROSA26)Sor*$^{CreERT2/+}$ (*[R258G]FlEx/+*) mES cells were treated with tamoxifen to generate *Acvr1*$^{[R206H]/+}$*; GT(ROSA26)Sor*$^{CreERT2/+}$ (*[R206H]/+*) and *Acvr1*$^{[R258G]/+}$*; GT(ROSA26)Sor*$^{CreERT2/+}$ (*[R258G]/+*) mES cells. The cells were treated with 10 nM Activin A, BMP2, ACVR1 Mab 2, or ACVR1 Fab 2 in various combinations for 1 hour. Activin A and ACVR1 Mab 2 but not ACVR1 Fab 2 induced Smad1/5/8 phosphorylation both in *[R206H]/+* and *[R258G]/+* mES cells, but not in *[R206H]FlEx/+* and *[R258G]FlEx/+* (i.e. wild type) mES cells. BMP2 (used as a positive control) induced Smad1/5/8 phosphorylation in *[R206H]FlEx/+*, *[R258G]FlEx/+*, *[R206H]/+*, and *[R258G]/+* mES cells.

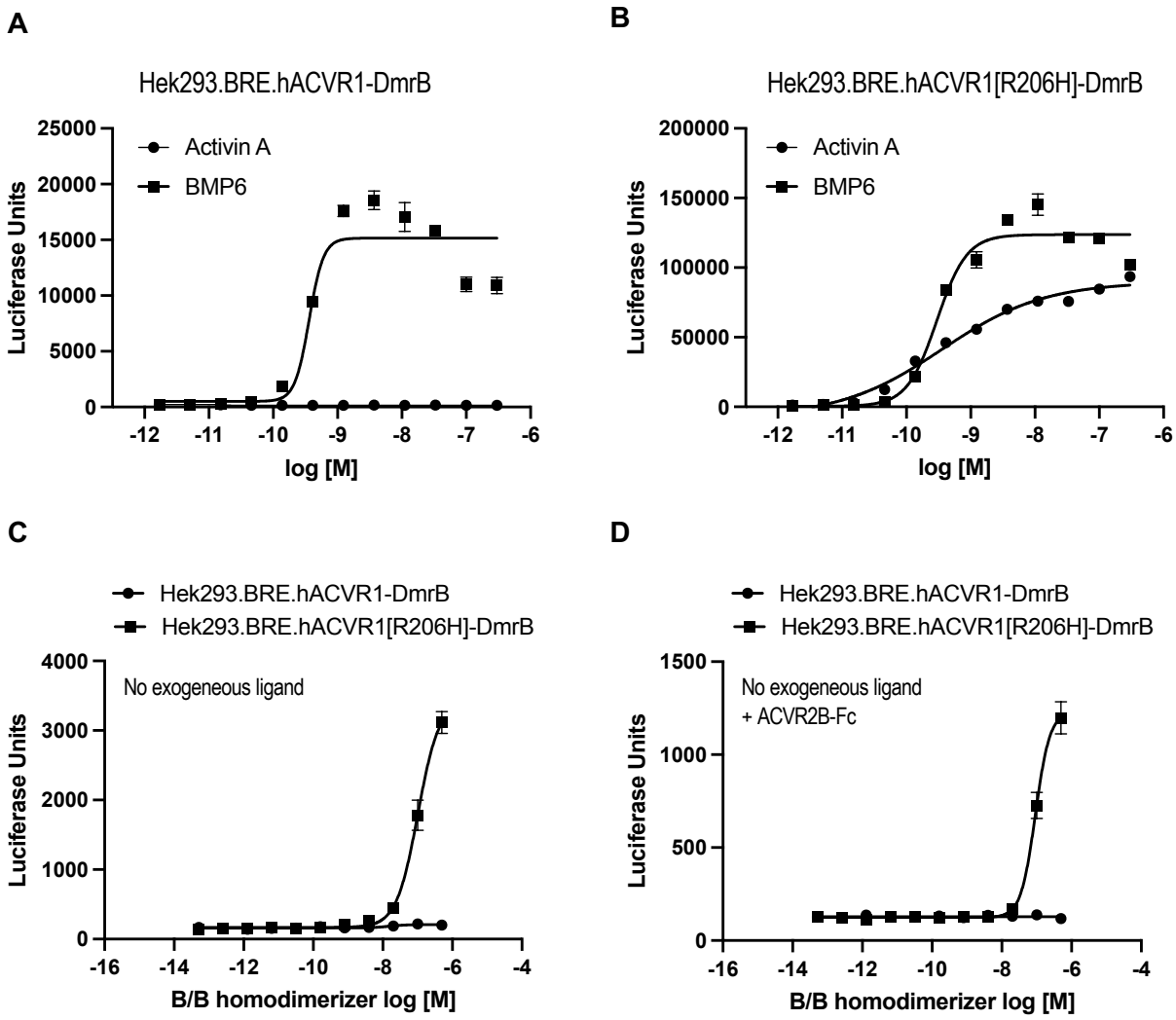

Supplemental Figure 6: Intracellularly driven dimerization of ACVR1[R206H], but not wild type ACVR1, induces Smad1/5/8 signaling.

Hek293 cells harboring P-Smad1/5/8 responsive luciferase reporter (BRE) were transfected with hACVR1-DmrB (**A**) or hACVR1[R206H]-DmrB (**B**). Homodimerization of C-terminal DmrB-tagged ACVR1 was induced with 20 nM B/B homodimerizer for 16 hours. Activin A activated Smad1/5/8 signaling only in hACVR1[R206H]-DmrB cells, but BMP6 activated Smad1/5/8 signaling both in hACVR1-DmrB and hACVR1[R206H]-DmrB cells (A-B). Intracellular homodimerization of hACVR1[R206H] activated Smad1/5/8 signaling in the absence of exogeneous ligands (**C**) as well as in the presence of 300 nM ACVR2B-Fc ligand trap (**D**).

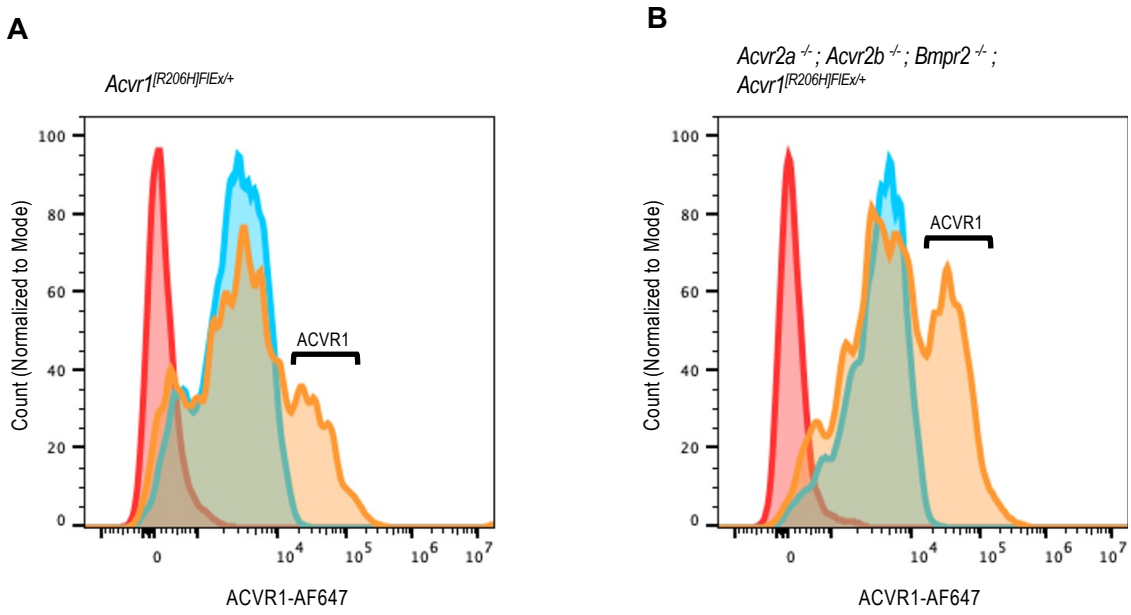

Supplemental Figure 7: Loss of *Acvr2a*, *Acvr2b* and *Bmpr2* does not affect the expression of ACVR1. *Acvr1*$^{[R206H]FlEx/+}$; *GT(ROSA26)Sor*$^{CreERT2/+}$ mES cells (**A**) and *Acvr1*$^{[R206H]FlEx/+}$; *GT(ROSA26)Sor*$^{CreERT2/+}$ mES cells lacking *Acvr2a*, *Acvr2b* and *Bmpr2* (**B**) were stained with an ACVR1 antibody and analyzed by flow cytometry. Both cell lines were positive for ACVR1 expression on the cell surface. Red curves represent unstained cells, blue curves represent only secondary antibody-stained cells, and yellow curves represent ACVR1 primary antibody plus corresponding secondary antibody-stained cells. Hence, ACVR1 is present on the membrane of *Acvr1*$^{[R206H]FlEx/+}$ mES cells as well as *Acvr1*$^{[R206H]FlEx/+}$ mES cells lacking *Acvr2a*, *Acvr2b* and *Bmpr2*.

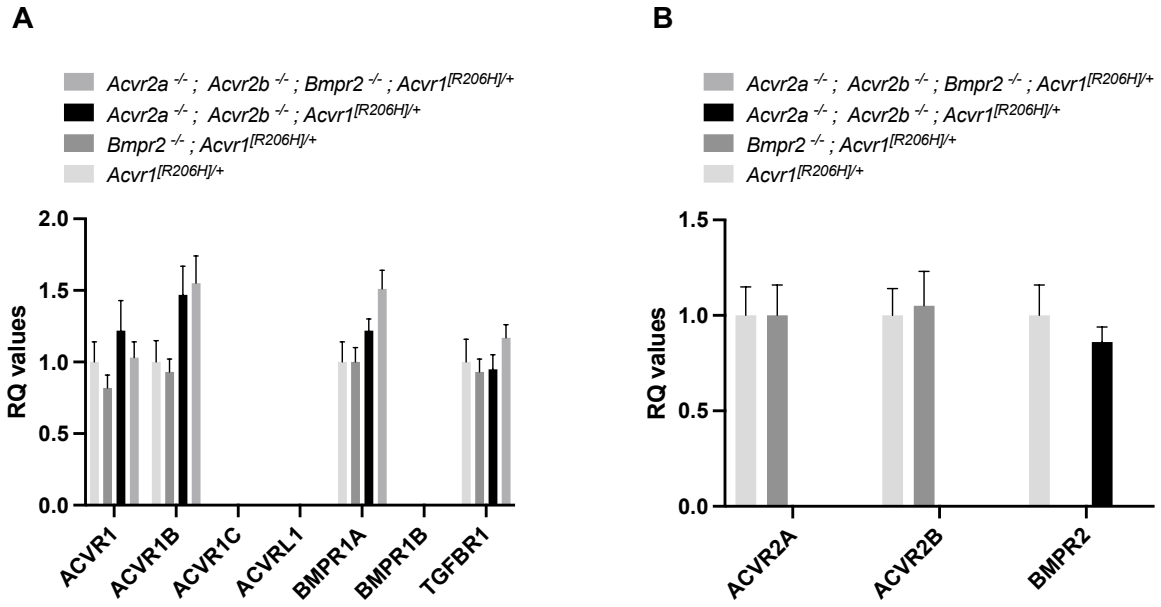

Supplemental Figure 8: TaqMan analysis of type II receptor KO mES cells.
Type I receptor (**A**) and type II receptor (**B**) mRNA levels in *Acvr1*$^{[R206H]/+}$*; GT(ROSA26)Sor*$^{CreERT2/+}$ mES cells wherein different combinations of *Acvr2a*, *Acvr2b* or *Bmpr2* have been knocked out. There is no significant difference between type I receptor mRNA levels of different type II receptor KO mES cells (**A**). Type II receptor mRNA levels remained unchanged in the different lines, except for loss of those type II receptors that have been knocked out (**B**).

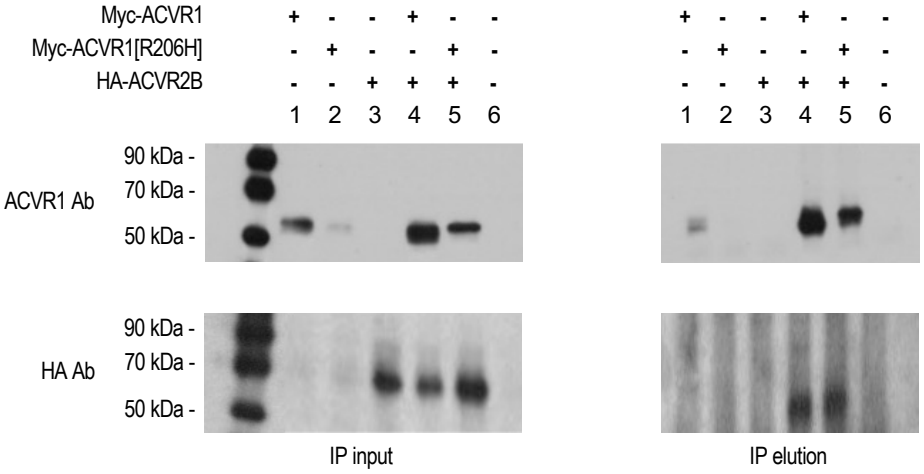

Supplemental Figure 9: ACVR1 forms heterocomplexes with ACVR2B in the absence of exogenous ligands and in the presence of ACVRIIB-Fc.

Hek293 cells were transfected with Myc-tagged ACVR1 and/or HA tagged ACVR2B. ACVR1 was immunoprecipitated using a myc antibody. ACVR1 and ACVR2B were detected using an ACVR1 antibody or HA antibody, respectively. ACVR2B immunoprecipitated with both ACVR1 and ACVR1[R206H] in the absence of exogenous ligands and in the presence of 300 nM ACVR2B-Fc.

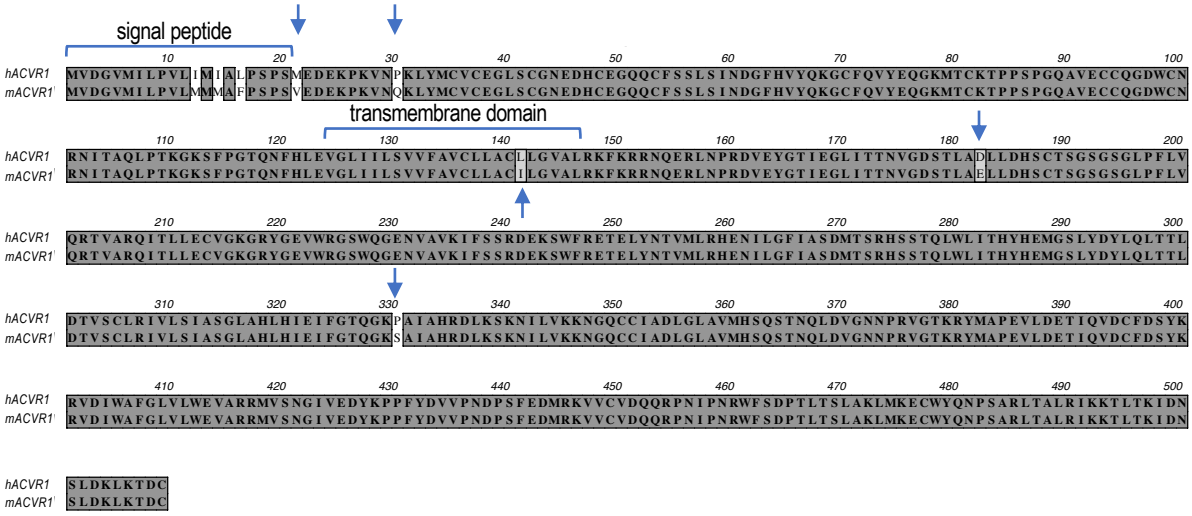

Supplemental Figure 10: Human ACVR1 differs from mouse ACVR1 by two amino acids in the intracellular domain.

Sequence alignment of human and mouse ACVR1. They differ by two amino acids in the extracellular domain (amino acids 21 and 30), one amino acid in the transmembrane domain (amino acid 141), and two amino acids in the intracellular domain (amino acids 182 and 330). The corresponding residues are indicated by blue arrow.

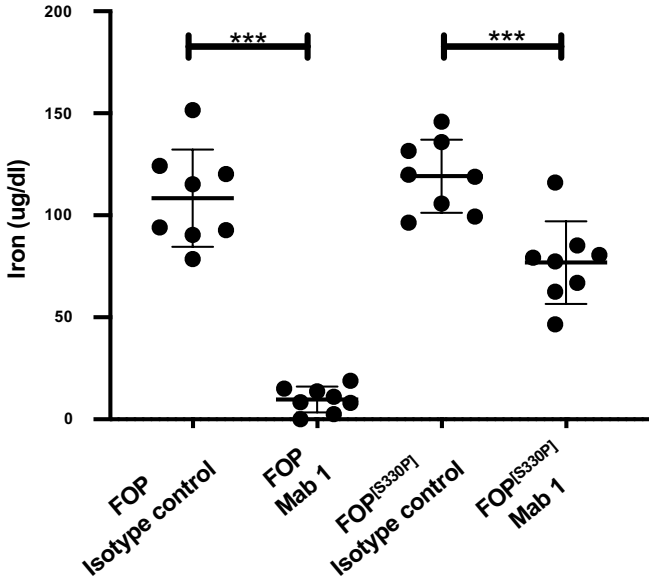

Supplemental Figure 11: ACVR1 Mab 1 reduces serum iron in both FOP and FOP[S330P] mice. *Acvr1[R206H]FlEx/+; GT(ROSA26)Sor$^{CreERT2/+}$* mice or *Acvr1huecto;[R206H]FlEx/+;[S330P]; GT(ROSA26)Sor$^{CreERT2/+}$* mice were injected with tamoxifen to initiate each model and generate FOP and FOP[S330P] mice, respectively. Both mouse lines were concurrently injected with ACVR1 Mab 1 or isotype control antibody at 10 mg/kg weekly. Serum iron was measured at 2 weeks post initiation. ACVR1 Mab 1 decreased serum iron compared to isotype control in both mouse models but to a lesser degree in FOP[S330P] mice. N= 8/group, data show the mean ± SD, *** $p<0.001$ t-test

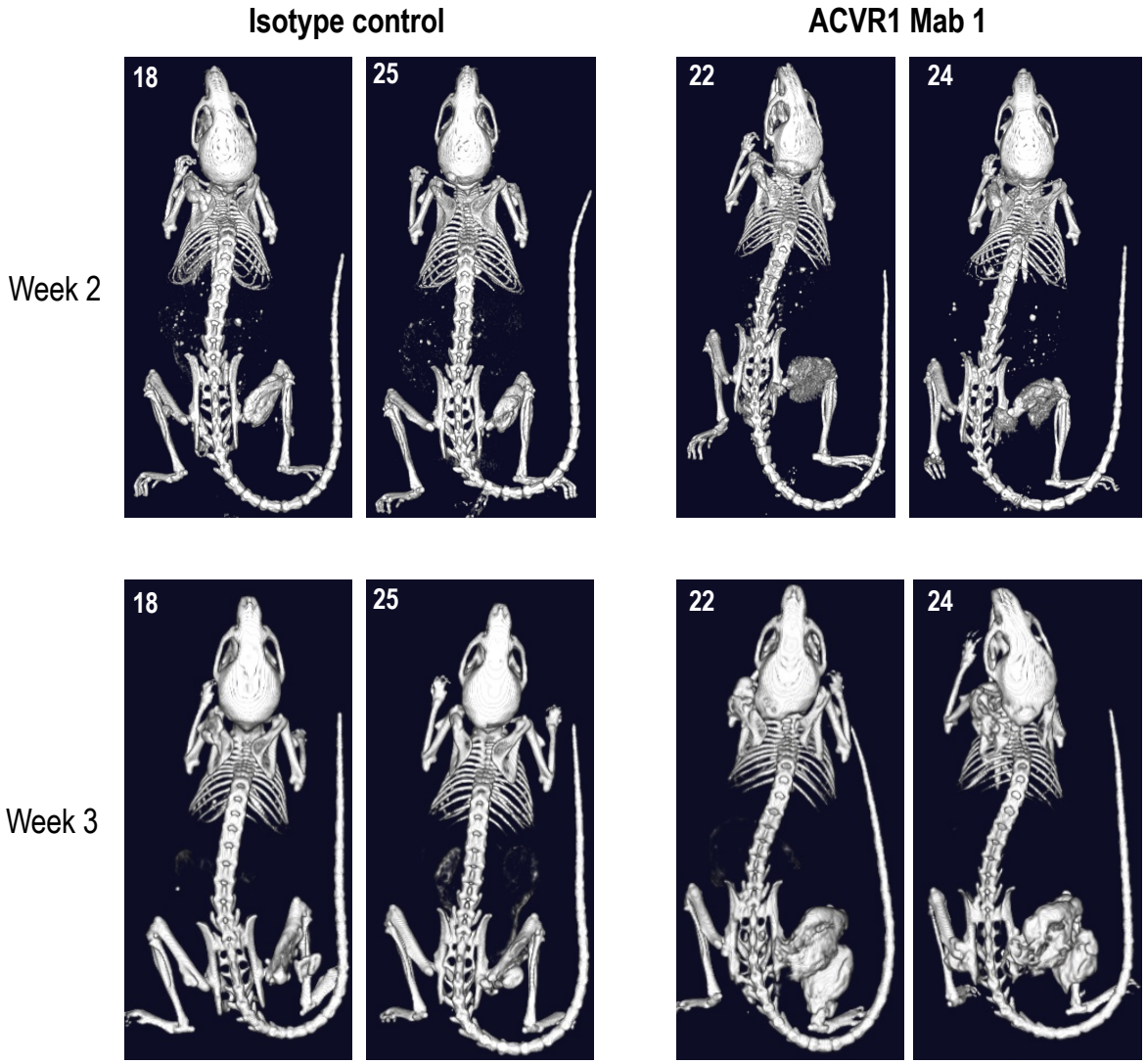

Supplemental Figure 12: ACVR1 antibodies alter the progression and amount of heterotopic bone formed in FOP mice.

Representative µCT images of FOP mice (*Acvr1*$^{[R206H]FlEx/+}$; *GT(ROSA26)Sor*$^{CreERT2/+}$ post-tamoxifen) treated with ACVR1 Mab 1 or isotype control antibody. At 2 weeks post initiation of HO, ACVR1 Mab 1 treated animals appears less mature than those treated with isotype control. By 3 weeks after model initiation, the heterotopic bone lesions formed in ACVR1 Mab 1 treated mice have matured and are much larger than those lesions observed in isotype Mab control treated mice.

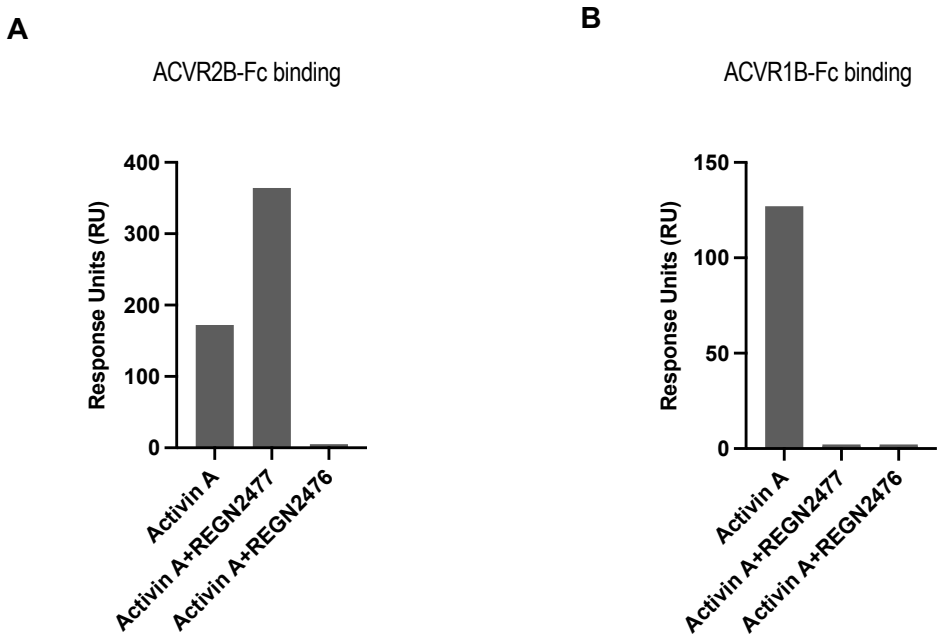

Supplemental Figure 13: REGN2476 blocks binding of Activin A to both type I and type II receptors, whereas REGN2477 only blocks binding of Activin A to type I receptors.
ACVR2B-Fc (**A**) and ACVR1B-Fc (**B**) were captured with an anti-human Fc antibody immobilized on a CM5 chip. 5 nM Activin A alone or in complex with REGN2476 and REGN2477 were injected over ACVR2B-Fc and ACVR1B-Fc at 37 ^{0}C. The association phase response units obtained by Activin A+/-REGN2476/REGN2477 binding to type I and type II receptors were showed in the graph. REGN2476 blocks binding of Activin A to both ACVR1B and ACVR2B, whereas REGN2477 only blocks binding of Activin A to ACVR1B (A-B).